Design of Q and W band feeds for Nanocosmos project

F. Tercero, O. García-Pérez

Technical Report IT2018-08

Observatorio de Yebes
19080 Guadalajara (Spain)
E-mail: f.tercero@oan.es

Abstract– WR22 and WR10 full waveguide band conical corrugated feeds are designed to work exceeding the standard bandwidth up to 31.5-50 GHz and 72-116 GHz. These feeds are part of the two systems considered for Nanocosmos project: the laboratory system and the 40 m radio telescope of the Yebes Observatory. Feed designs have been optimized with our own genetic algorithm to fulfill Gaussian beam waist parameters of 15 and 11 mm for Q and W bands respectively, low port reflection and high aperture efficiency for the 40 m radio telescope with the additional optics.

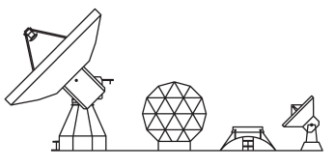

Contents

1 Introduction

One of the aims of the Nanocosmos project is to develop a simulation gas chamber with low pressure gases inside, in order to emulate the circumstellar dust formation. These gases can be observed in-situ using radio astronomical receivers, which results advantageous in terms of spectral resolution and sensitivity. These experiments will be complemented by high resolution astronomical observations with the 40 m radio telescope, in which Q and W band receivers must be upgraded to provide wider bandwidth and better spectral resolution. The development of this instrumentation is also a key aspect of the Nanocosmos proposal [1].

The simulation gas chamber, also named *gas-cell* or *laboratory system*, is a simultaneous Q and W band receiver with single linear polarization and bandwidths (31.5-50 GHz and 72-116 GHz) exceeding the standard WR22 and WR10 rectangular waveguide specifications. This dual-band receiver looks at a cryogenic cold load at 20 K through an optical system, and spectral Observations can be performed when the gas chamber is settled at the middle of the system [2].

On the other hand, the new receivers for the 40 m radio telescope the feed horns (placed at the secondary focus of the radio telescope) are coupled to the sub-reflector by means additional optics in the cassegrain focus. In this system the two receivers are in different dewars, each of them providing dual linear polarization [3].

Both optical systems (laboratory and radio telescope) can be designed in such a way that the horn feeds are identical. This assumption does not affect the performance and it simplifies the horn design. This report presents the design and characterization results of the Q and W band horn antennas for the Nanocosmos systems.

2 Specifications

Basic optical and mechanical specifications for the design of both Q and W band feed horns are showed in Table 1 and Table 2 respectively. The beam waist has to be at a fixed position, and close to the aperture, for the entire bandwidth. This is required to illuminate the focused broadband systems without the help of any additional refractive element. The specification also looks for an implementation as compact as possible.

Input waveguide radius	a	mm	6.00	Compatible with available OMT [4]
Input reflection (max.)	s_{11}	dB	-20	
Beam waist	w0q	mm	15	
Beam waist position	z0q	mm	0	With respect the aperture
Diameter	D	mm	minimal	
Slant length	L	mm	minimal	
Flange type			square	Non-precision. Similar to UG599 but NOT a rectangular waveguide WR22 output
Support structure	Ds	mm	46	Attach it with cylindrical clamp thickness=12mm
Distance from support structure to aperture	ds	mm	96	

Table 1. Specifications for the Q-band feed.

Input waveguide radius	a	mm	2.74	
Input reflection (max.)	s_{11}	dB	-20	
Beam waist	w0q	mm	11	
Beam waist position	z0q	mm	0	With respect the aperture
Diameter	D	mm	minimal	
Slant length	L	mm	minimal	
Flange type			round	Non-precision. Similar to UG587 but NOT a rectangular waveguide WR10 output
Support structure	Ds	mm	36	Attach it with cylindrical clamp thickness=12mm
Distance from support structure to aperture	ds	mm	83	

Table 2. Specifications for the W-band feed.

3 Feed Design

3.1 Electrical design and optimization

The optimized profiles for the Q and W band horn antennas are showed in Fig. 3.1.

The throat section has been designed to have smooth transition from a conical waveguide to the corrugated one. As it is explained in [5], groves in corrugated feed starts with a small slot that is gradually increased to the final slot. On the other hand, the radiation section is based on a profiled corrugated feed in order to obtain a compact feed size and the beam waist fixed across the bandwidth.

The profiles are not defined analytically, but using NURBS (Non Uniform Rational Bezier Spline) curves instead. NURBS allow having arbitrary shapes formed by low order joined curves that are defined by several control points. Therefore, each feed is parameterized with a single set of parameters which completely defines the structure.

The electrical performance of the feeds has been optimized using a genetic algorithm based on NSGA-II [6], which classifies the population of individuals in hierarchical groups of non-dominated individuals. The individuals in the highest groups (those that they are not dominated by anyone) are the candidates to be a good compromise solution in all evaluated tests (s_{11}, beam waist and aperture efficiency) simultaneously.

For the algorithm, the feeds are evaluated using different tools. Firstly, a commercial modal-matching code [7] is used to estimate input reflection, aperture fields and radiation patterns in the bandwidth. Then, beam waist size and position is obtained from the aperture fields, and global aperture efficiency has been calculated using a quasi-optical model of the 40 m radio telescope assuming fundamental Gaussian beam mode.

After the evaluation, the feed is geometrically and electrically defined by the list of geometrical parameters and the evaluated figures (s_{11}, beam waist and radio telescope efficiency). The full list of numbers (parameters and evaluation figures) is called as the chromosome of the individual because it has its genes and also gives information about its performance in the optical system.

The simulated results obtained from the optimized Q and W band feed horns are showed in Fig. 3.5-Fig. 3.9. Beam waist size and position values are slightly different than to those given by the specification. Nevertheless, the estimated aperture efficiency is about 79% in both bands, which is high enough for this application.

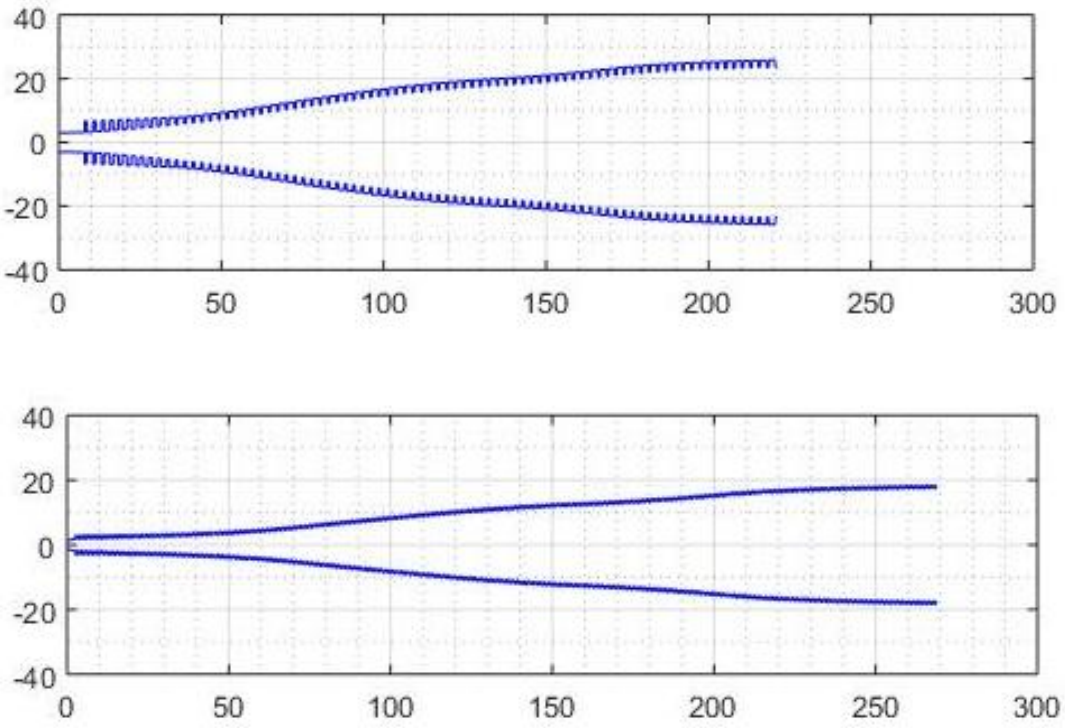

Fig. 3.1. Final Q band and W band horn feed profiles (dimensions in mm).

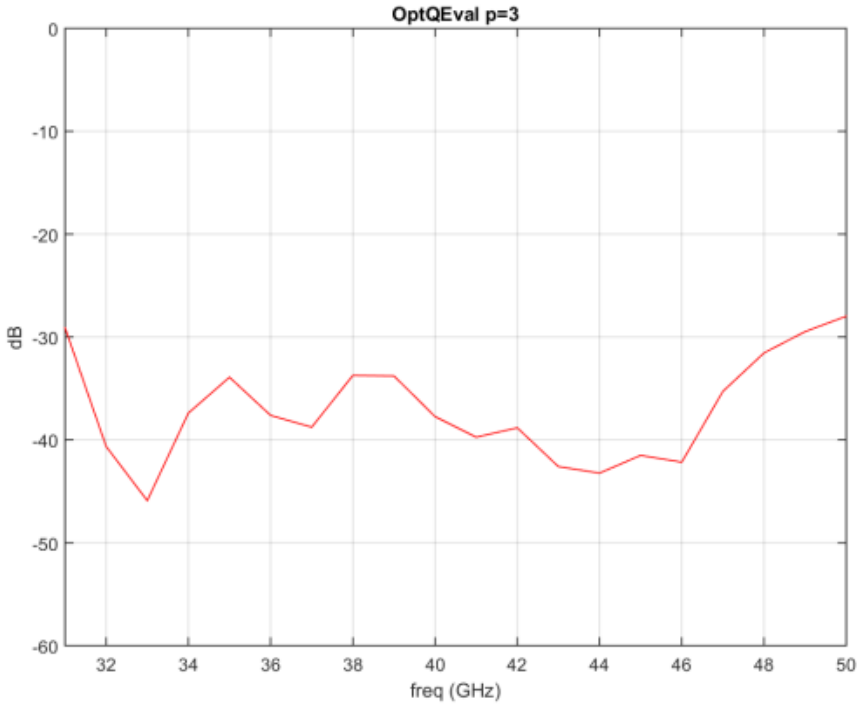

Fig. 3.2. Simulated results of the Q band feed horn input port reflection

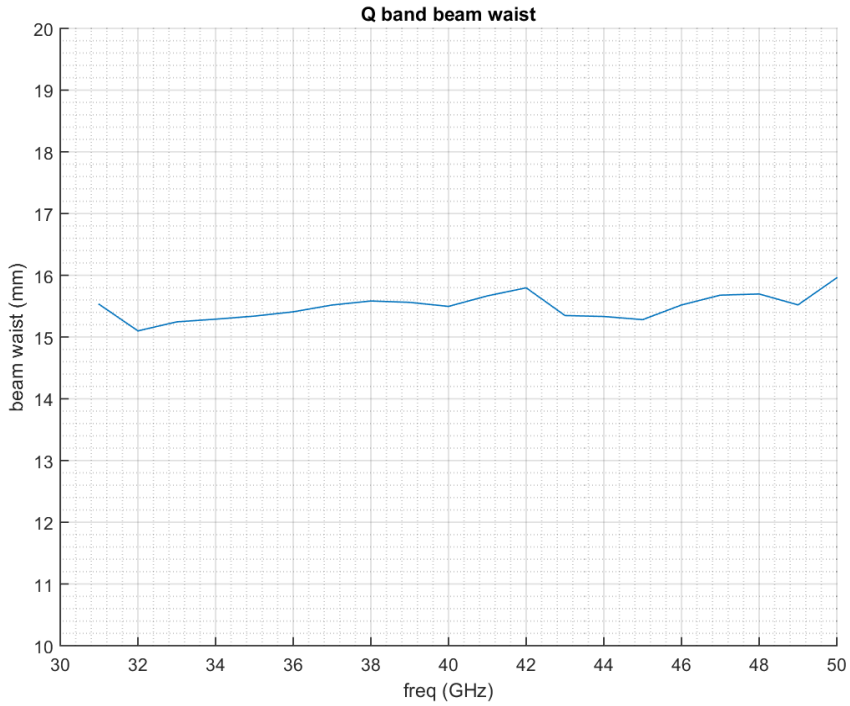

Fig. 3.3. Simulated results of the Q band feed horn beam waist size

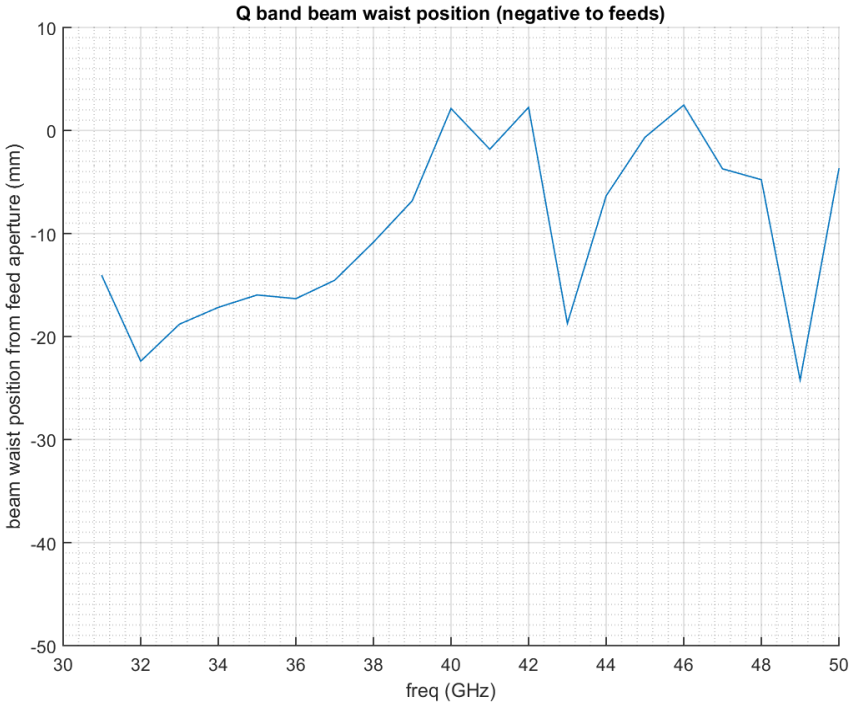

Fig. 3.4. Simulated results of the Q band feed horn beam waist position

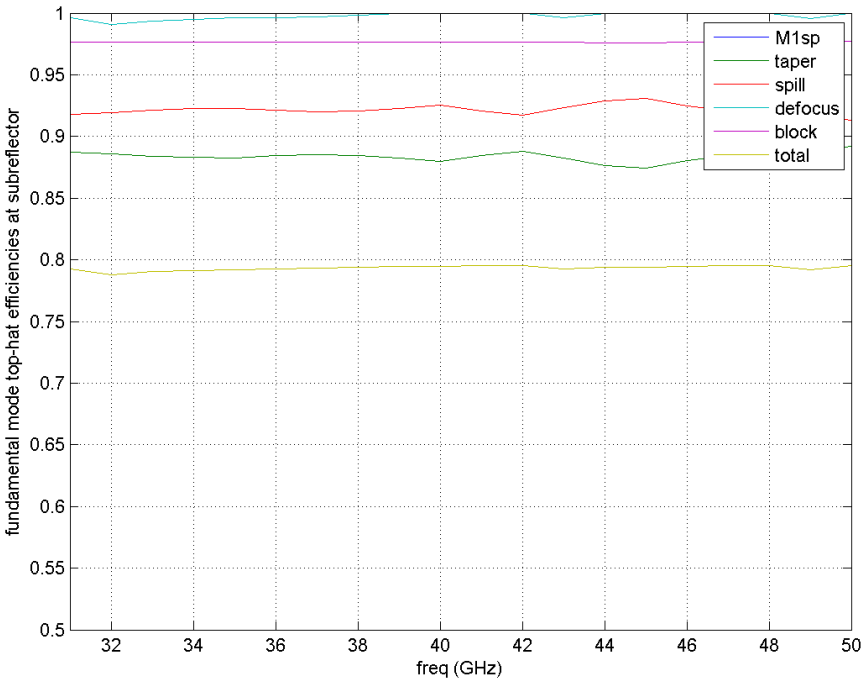

Fig. 3.5. Simulated results of the Q band feed horn aperture efficiency over the radio telescope.

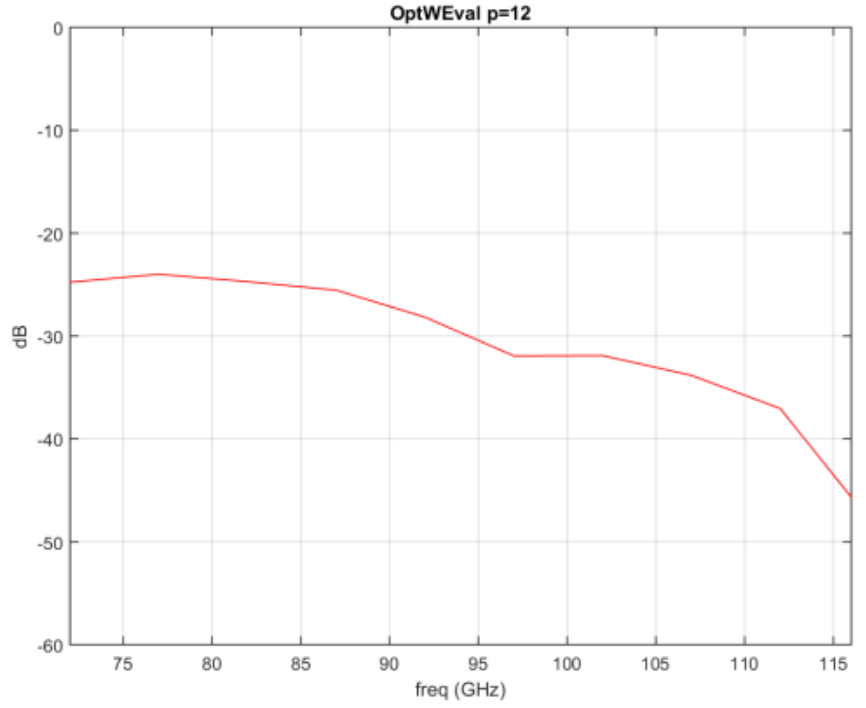

Fig. 3.6. Simulated results of the W band feed horn input port reflection

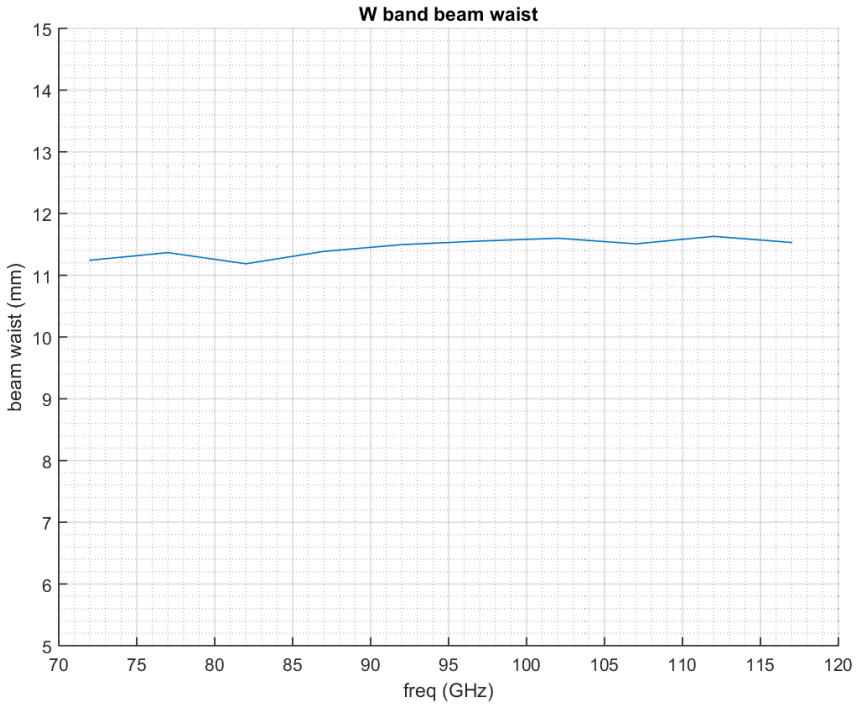

Fig. 3.7. Simulated results of the W band feed horn beam waist size

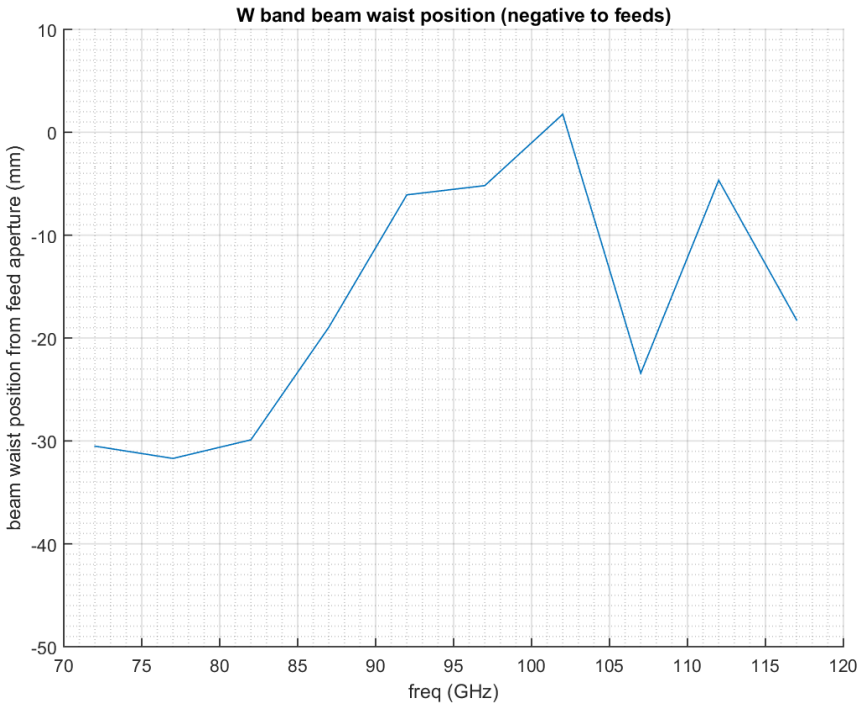

Fig. 3.8. Simulated results of the W band feed horn beam waist position

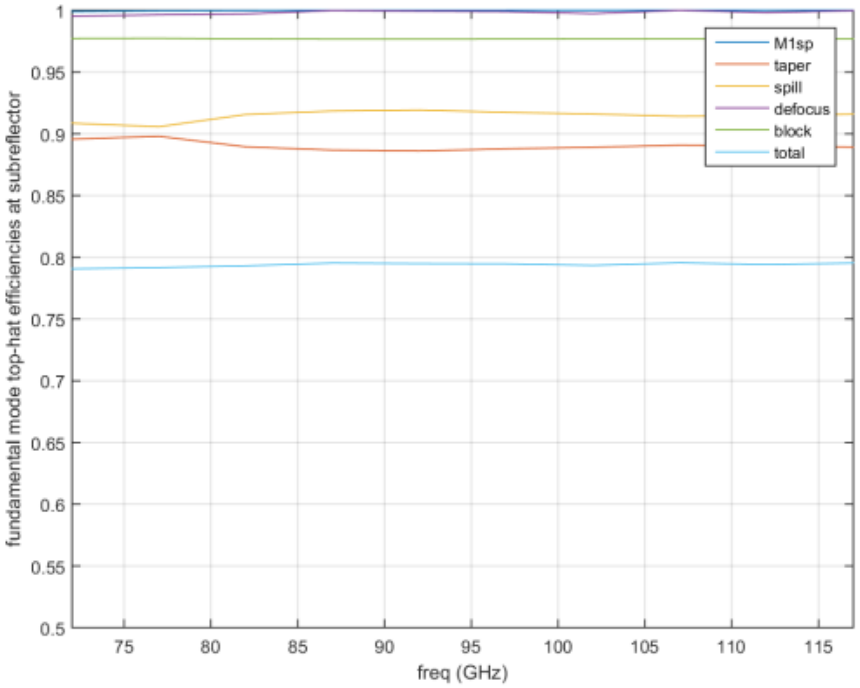

Fig. 3.9. Simulated results of the W band feed horn aperture efficiency over the radio telescope.

3.2 Mechanical design

The manufacturing drawings of the Q band feed horn are showed in Fig. 3.10. A cylinder shaped flange of 46 mm of diameter and 12 mm of length has been added at 96 mm far from the aperture. This will be used to attach the feed to the cryostat. The waveguide flange is compatible with WR22 square flange UG599. Threads are UNC-4-40. Additional 2 mm centering pins are drilled in the flange.

The manufacturing drawings of the W band feed horn are showed in Fig. 3.11. As in the Q-band design, a cylinder shaped flange of 36 mm of diameter and 12 mm of length has been added at 83 mm far from the aperture. The waveguide flange is compatible with WR10 square flange UG387. Threads are UNC-4-40. Additional centering pins holes are drilled in the flange. Although, holes are ready for fixed pin insertion (in the 1.56 mm hole), the pins were not mounted.

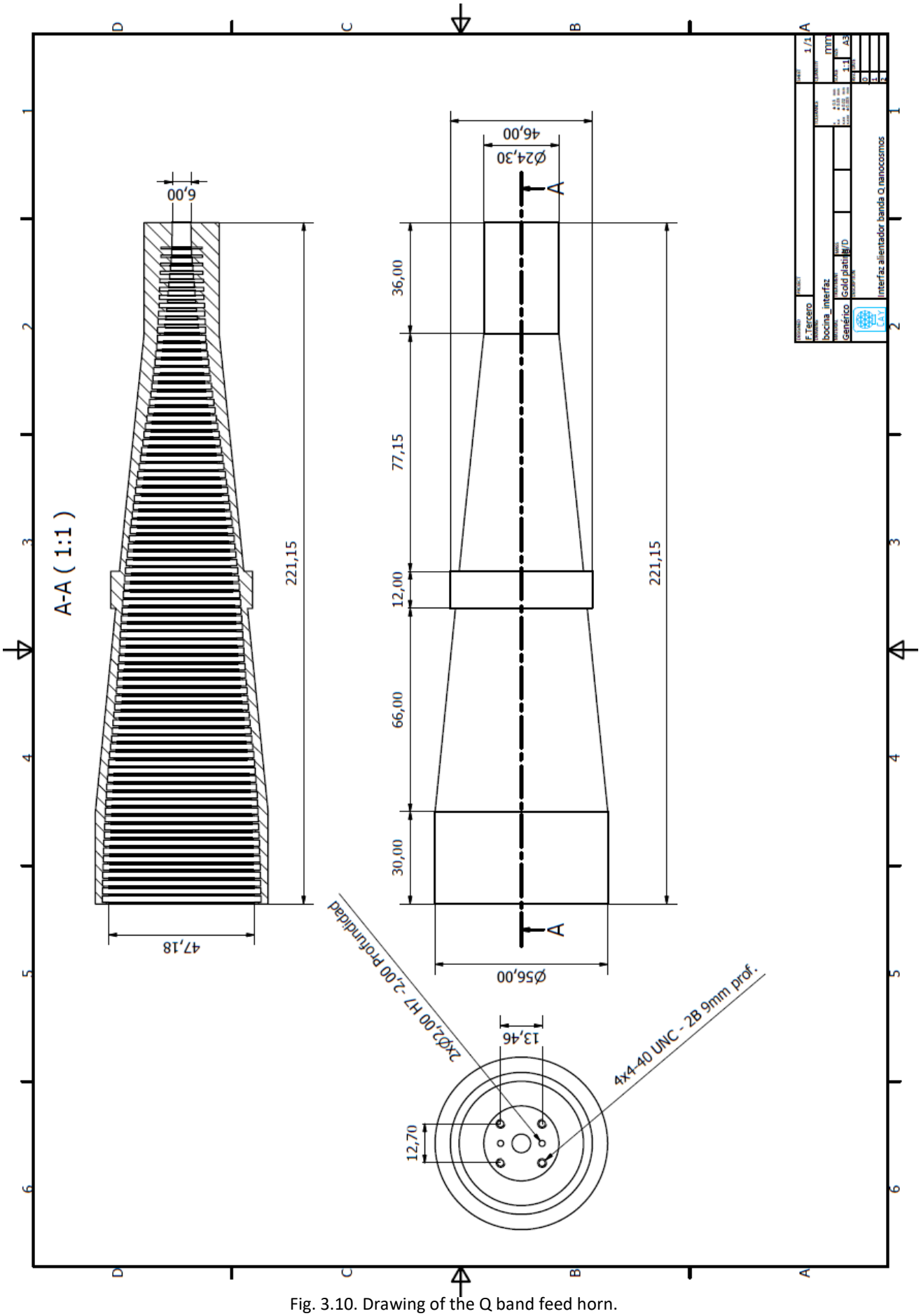

Fig. 3.10. Drawing of the Q band feed horn.

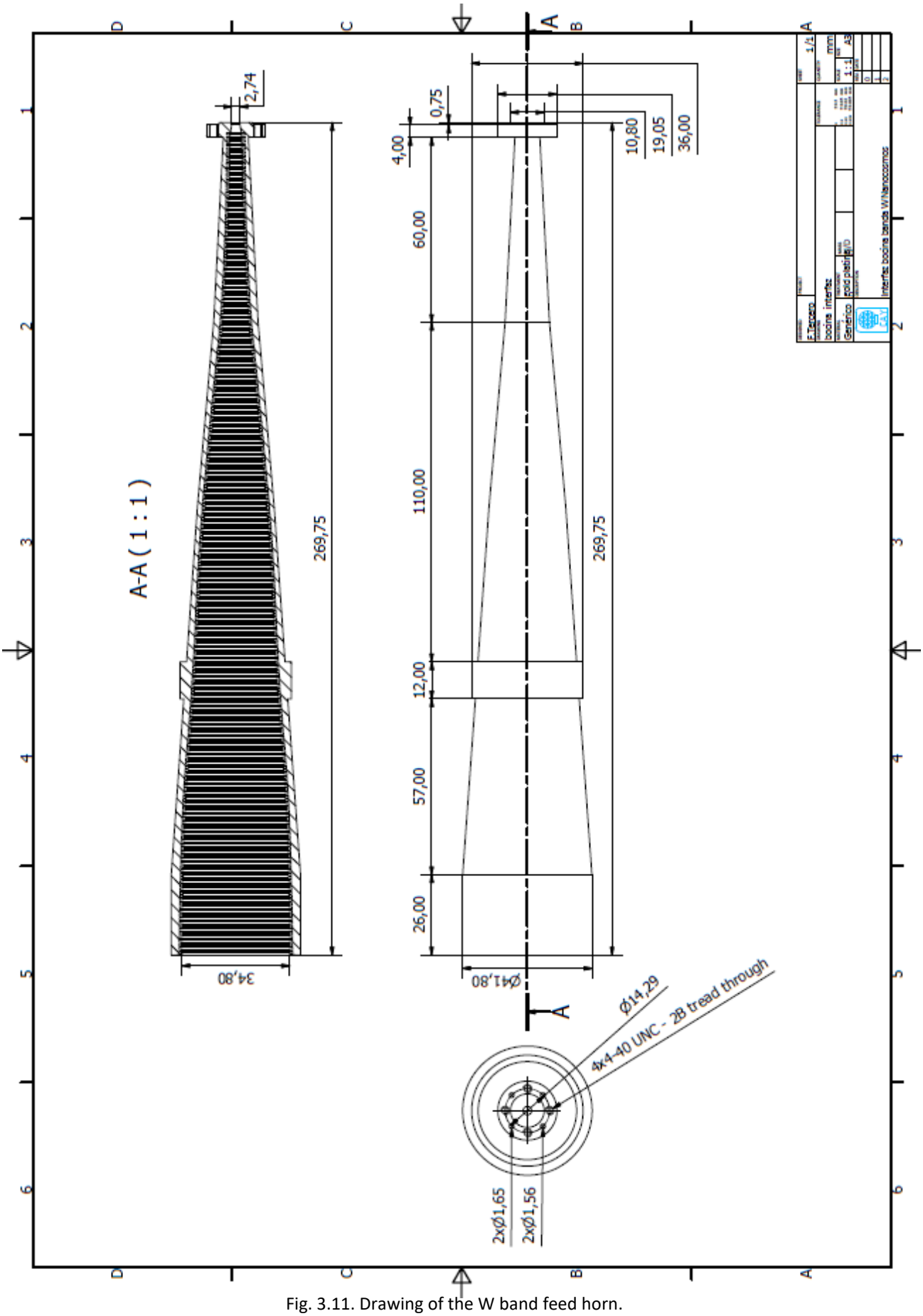

Fig. 3.11. Drawing of the W band feed horn.

4 Feed Fabrication

Two units of each feed antenna design have been manufactured by Thomas Keating Company in UK [8] (see Fig. 4.1). They were fabricated by electroforming technique, using copper with a thin layer of gold as electroformed material. The plating in the inner side of the feed does not seem as good as in the outside. The inside plating was done previously to the cooper deposition while the outside plating must be done after of the machining of the cooper. Some of the threaded drills seemed not work very fine, so it was necessary to redo the tread softly. It was probably due to the last outer plating. General aspect and tolerances were very good as well as the machining quality.

Since the feeds (circular waveguide) are going to be connected either to a standard rectangular waveguide, in the case of the laboratory system, or to a square waveguide, in the case of the orthomode transducers for the radio telescope receivers, additional transitions were also required. The drawings of the rectangular to circular transitions can be found in Appendix A and Appendix B. Their respective lengths are 46 mm for the WR22 waveguide and 37.5 mm for the WR10 waveguide.

Fig. 4.1. In the picture, four feeds as part of the shipment from Thomas Keating.

5 Feed Measurements

5.1 Q band port reflection

The reflection coefficient of the Q band feeds was directly measured at the circular waveguide port. A custom TRL calibration kit has been used, and the measured data have been smoothed by 7%. The comparison between measured and simulated return loss for each fabricated unit is showed in Fig. 5.1.

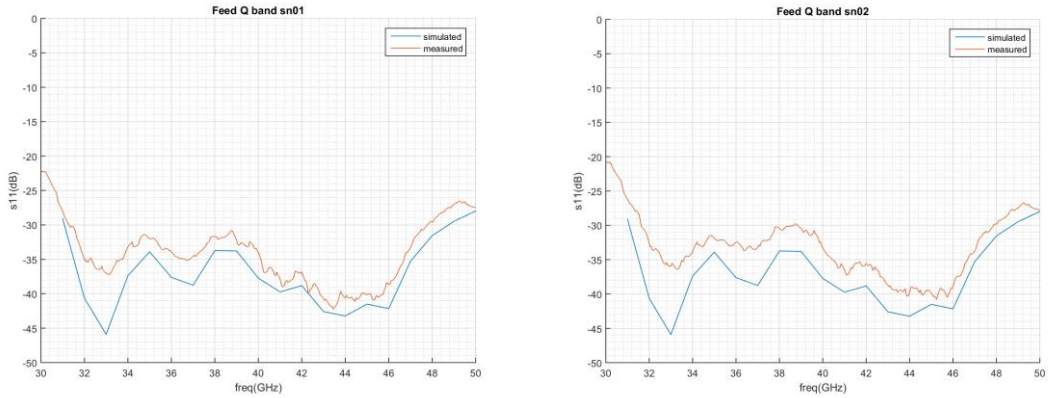

Fig. 5.1. Measured and simulated port reflection loss of the Q-band feeds.

5.2 W band port reflection

In the case of the W-band feeds they were measured using a circular to rectangular transition (Appendix B). The PNA frequency range was extended up to 70-120 GHz using two OML millimeter-wave heads. The maximum frequency specified for the heads is 110GHz, so the measurements obtained between 110 and 120 GHz can be inaccurate. Standard TRL calibration has been applied at the rectangular waveguide port, and the measured data have been smoothed by 7%. The comparison between measured and simulated return loss for each fabricated unit is showed in Fig. 5.2. Ripple over the band is due to the 36 mm rectangular to circular waveguide transition.

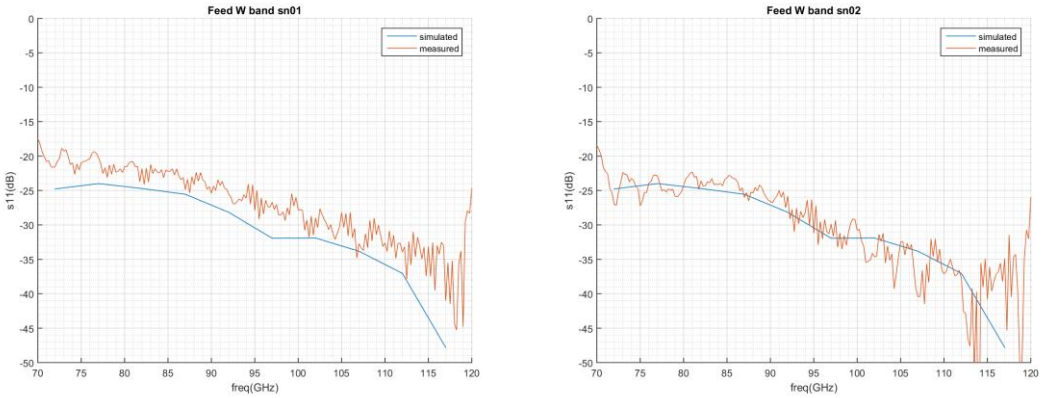

Fig. 5.2. Measured and simulated port reflection loss of the W-band feeds.

5.3 Q band radiation patterns

The measurement of the radiation patterns of the Q band feeds were performed for single linear polarization, by using WR22 transition to feed the antenna. The accuracy of the pointing between the AUT holder and the open waveguide probe was better than 0.025 deg.

In addition to the AUT pointing, polarization axis of the AUT must be aligned with the probe polarization axis (roll axis). It was done mechanically in a workshop table, using a vertical gauge, where the flat side of the square waveguide and the gauge are set parallel.

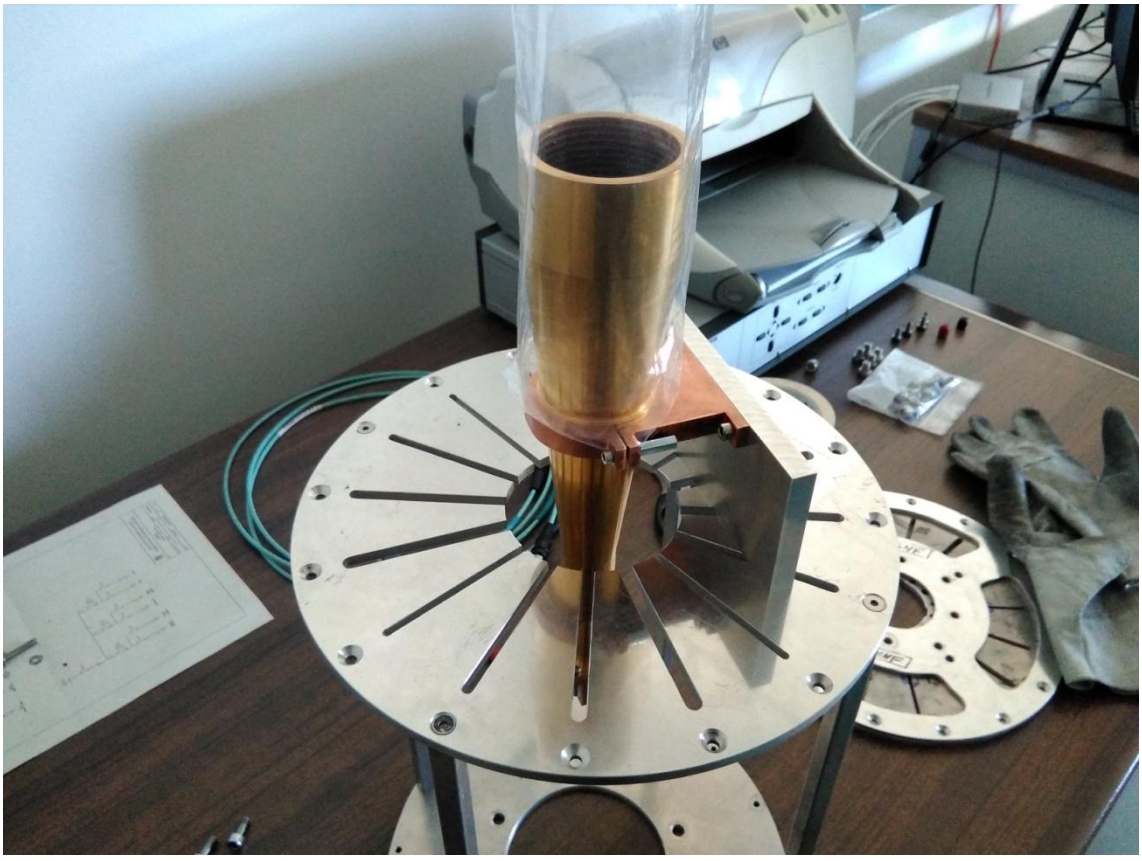

Fig. 5.3. Mechanical holder of the anechoic chamber and additional clamping interface (cooper) of the feed.

Pointing error was higher than expected with previous mechanical alignment. Feed was fixed to the anechoic chamber holder with an additional interface piece which it could not be accurate enough. New interface was designed for the final integration stage (cooper piece in Fig. 5.3). Pointing error was less than 1 deg (0.2 std. deviation) in the whole bandwidth in this measurement campaign. Mean value of the pointing was calculated to correct the radiation patterns showed in this report.

The complete set of measured radiation patterns of both Q band horn antennas are plotted in Appendix C and Appendix D. In order to show the excellent agreement between measured and simulated results, the radiation pattern at 40GHz is presented in Fig. 5.4, even which the cross-polar level agrees rather well.

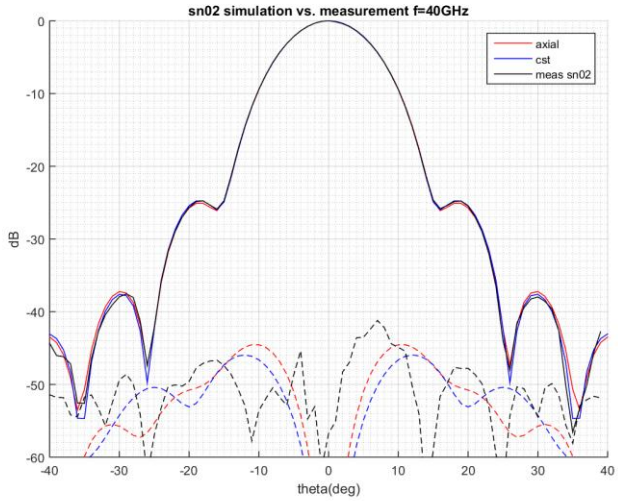

Fig. 5.4. Measured and simulated (axial and CST) radiation patterns (diagonal cut plane) of the Q-band feed (sn02) at 40 GHz.

5.4 W band radiation patterns

For the W-band measurements, OML mm-heads were used to downconvert the radiated frequencies into lower-frequency signals that can be processed by the PNA. The mm-head is bulky, which makes more complicated the alignment of the feed. In this case the feed and mm-head was electrically aligned finding the maximum from horizontal and vertical cuts before the definitive measurement. This procedure provides nicely aligned patterns, but the mechanical error cannot be evaluated and controlled. As measurement probes are leveled, the alignment of the polarization axis is done by means of leveling the mm-head.

The complete set of measured radiation patterns of both W band horn antennas are plotted in Appendix E and Appendix F. The comparison between the measured and simulated pattern at 100 GHz is presented in Fig. 5.5.

In this case, the measured patterns were properly aligned, so no additional correction was needed. The cross-polar levels at the axis are acceptable, but they are worse than in the Q-band feed. This can be attributable to manufacturing or leveling inaccuracies. The measurement of the side lobes above 115 GHz is also inaccurate due to the limited sensitivity of the instrumentation at so high frequencies.

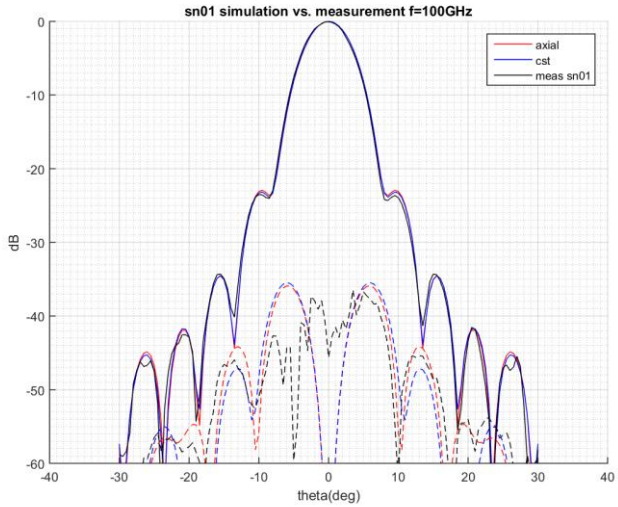

Fig. 5.5. Measured and simulated (axial and CST) radiation patterns (diagonal cut plane) of the W-band feed (sn01) at 100 GHz.

5.5 Q band phase center

The location of the phase centre of the Q band horn feeds obtained from the measured radiation patterns is plotted in Fig. 5.6. This position has been defined with respect to the aperture, in such a way that negative values are inside the horn.

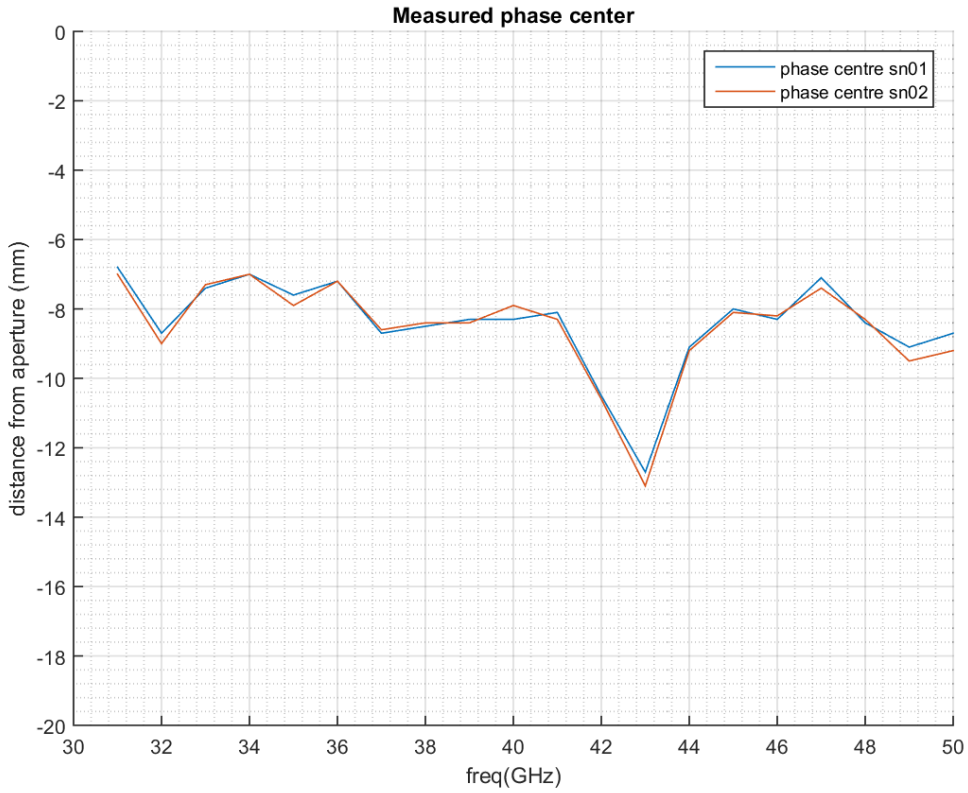

Fig. 5.6. Measured phase centre for Q-band feeds.

5.6 W band phase center

The measured phase centre and expected beam waist of the W band horn feeds are showed in Fig. 5.7. In this case, measurements above 110 GHz should be carefully considered because the instrumentation is out of specification.

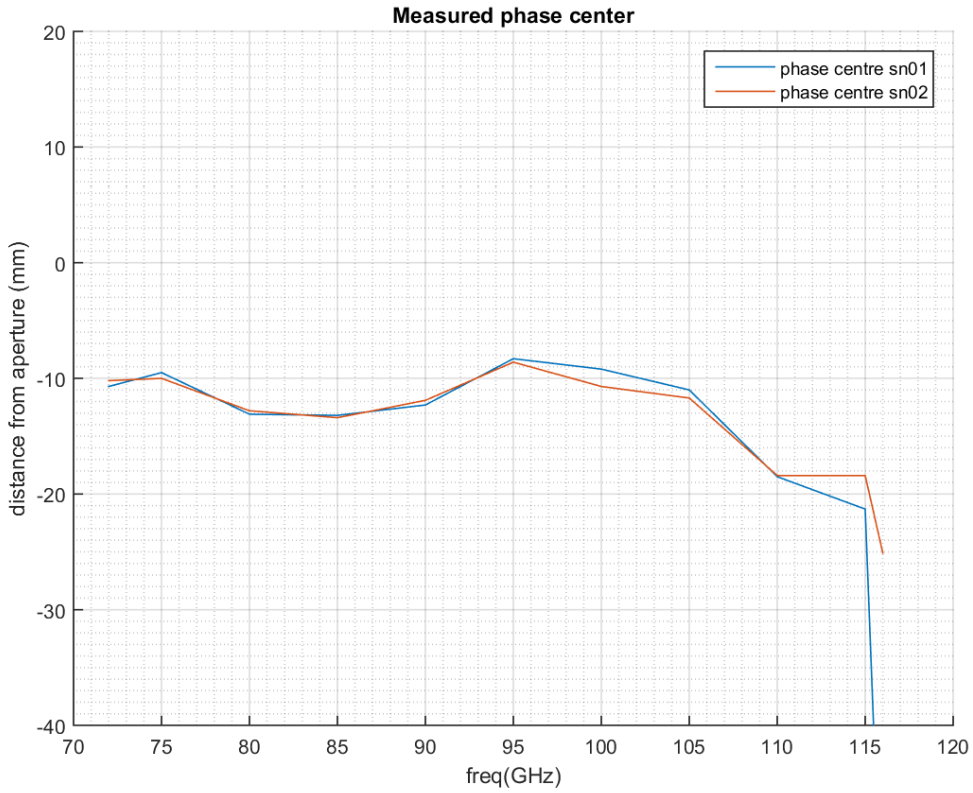

Fig. 5.7. Measured phase for the W-band feeds.

6 Conclusions

Corrugated conical feeds for the Nanocosmos project have been designed and built. Experimental results reveal excellent agreement compared to simulations, even with cross-polar levels below -40dB. Beam waist position varies between +5mm/-20mm for the Q band and between 0mm/-30mm for the W band. Although this does not fulfill the preliminary specification of fixed beam waist, it does not seem to have serious effect on the aperture efficiency of the radio telescope, which is estimated to be almost 80% for both optical systems.

References

[1] Nanocosmos project. [Online]. Available: https://nanocosmos.iff.csic.es/

[2] F. Tercero, "Optical system of Nanocosmos Laboratory Receiver," *Technical Report* (in preparation).

[3] F. Tercero, "Optical system of Q and W band receivers in 40 m radiotelescope," *Technical Report* (in preparation).

[4] S. Lopez-Ruiz et al., "31.5 GHz - 50.0 GHz Ortho-Mode Transducer for the Nanocosmos Receiver in the 40m Radiotelescope," Technical Report IT-CDT-2017-01, 2017. [Online]. Available: http://www1.oan.es/reports/doc/IT-CDT-2017-1.pdf

[5] X. Zhang, "Design of Conical Corrugated Feed Horns for Wide-Band High-Frequency Applications," *IEEE Transactions on Microwave Theory and Techniques*, vol. 41, no. 8, pp. 1263, Aug. 1993.

[6] N. Srinivas and K. Deb, "Muiltiobjective optimization using nondominated sorting in genetic algorithms," *Evolutionary Computation*, vol. 2, no. 3, pp. 221–248, 1994.

[7] AXIAL. [Online]. Available: http://www.smtconsultancies.co.uk/

[8] Thomas Keating Ltd. [Online]. Available: http://www.terahertz.co.uk/

Appendix A. WR22 to 6 mm round transition.

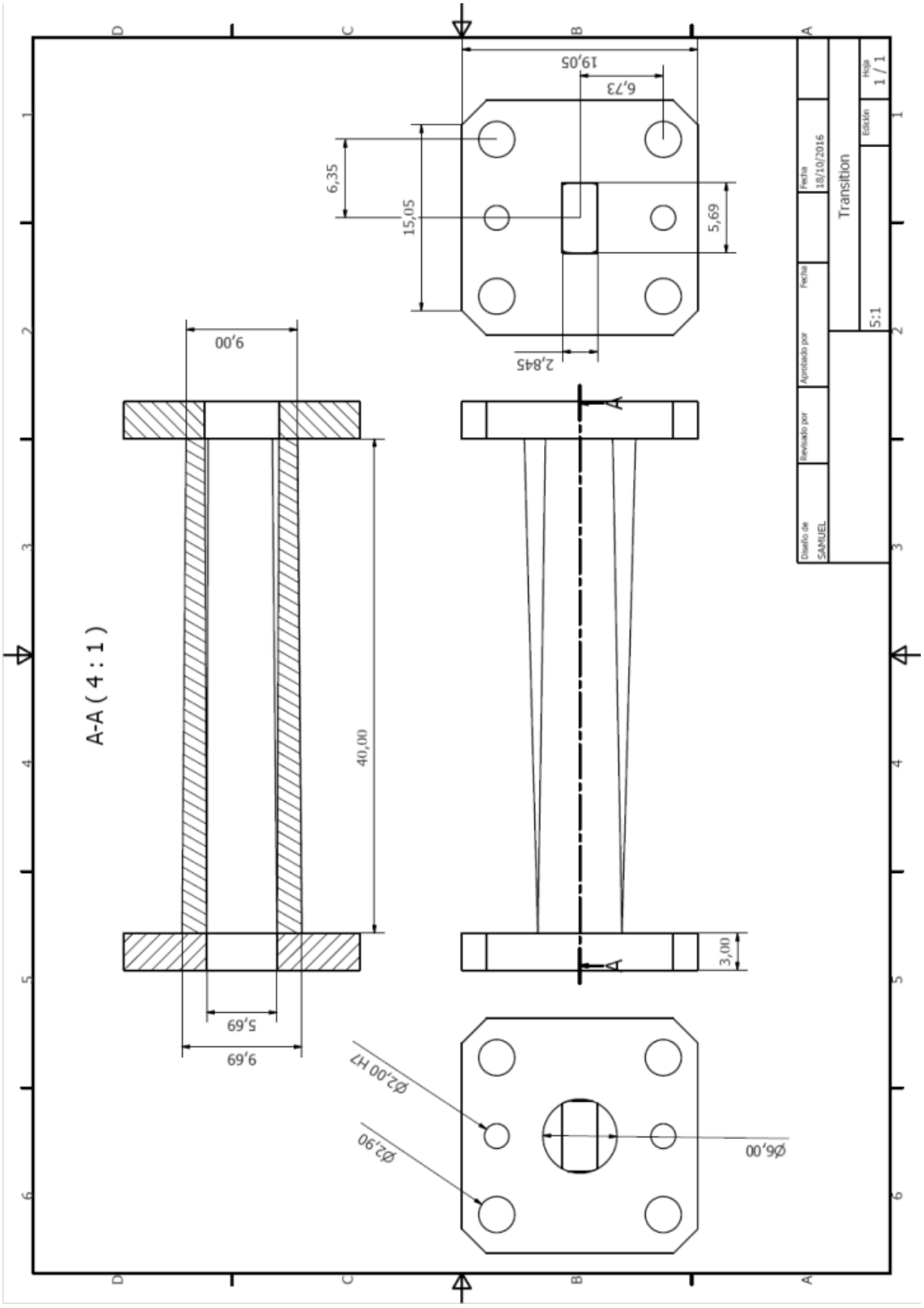

Appendix B. WR10 to 2.74 mm round transition.

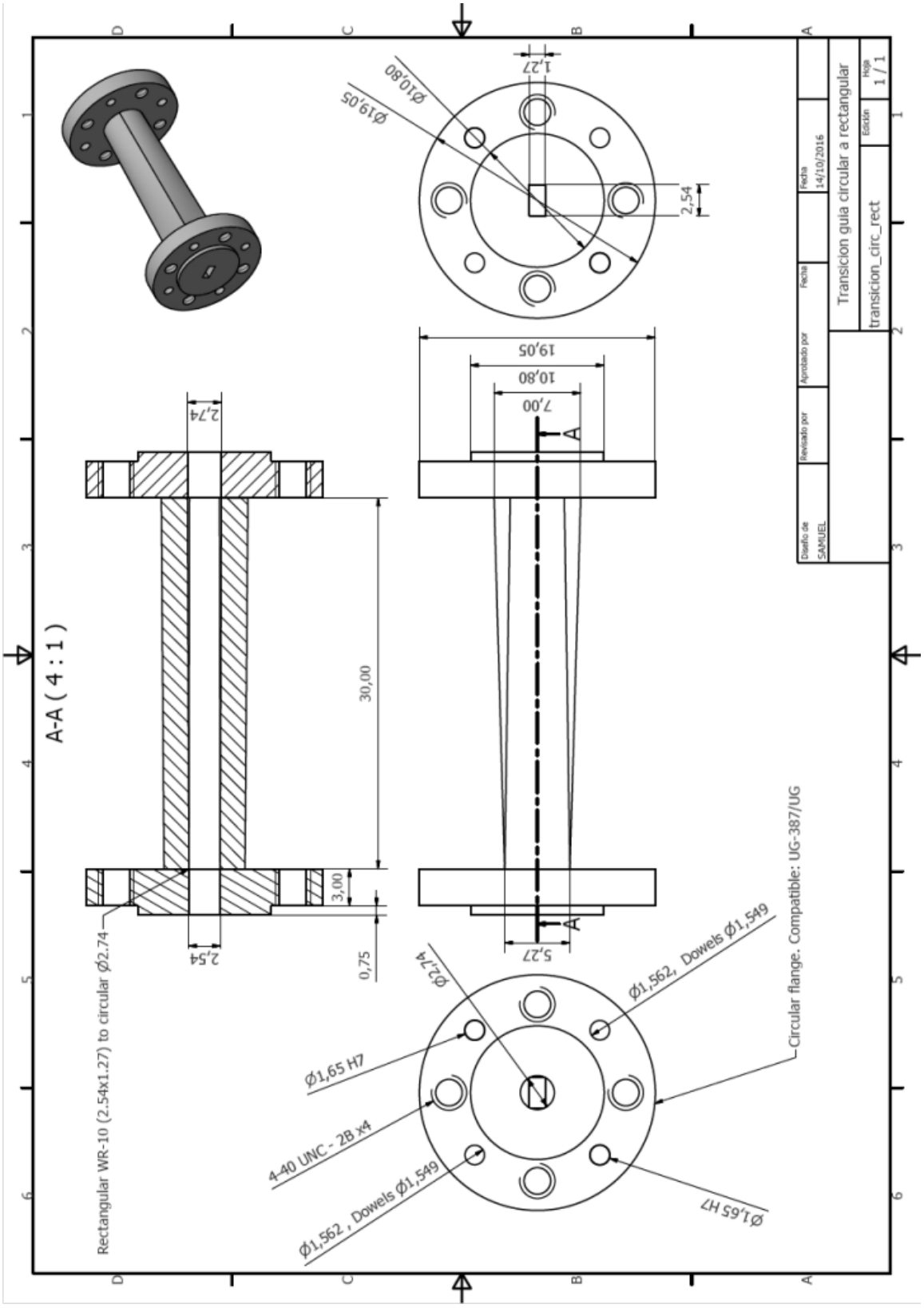

Appendix C. Q-band radiation patterns sn01

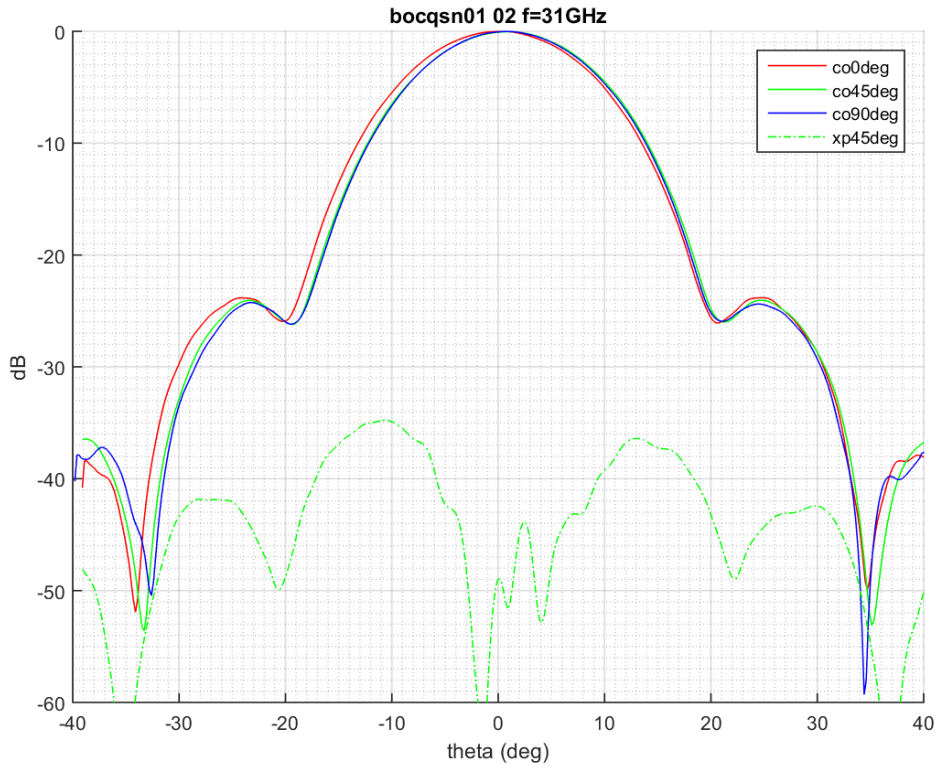

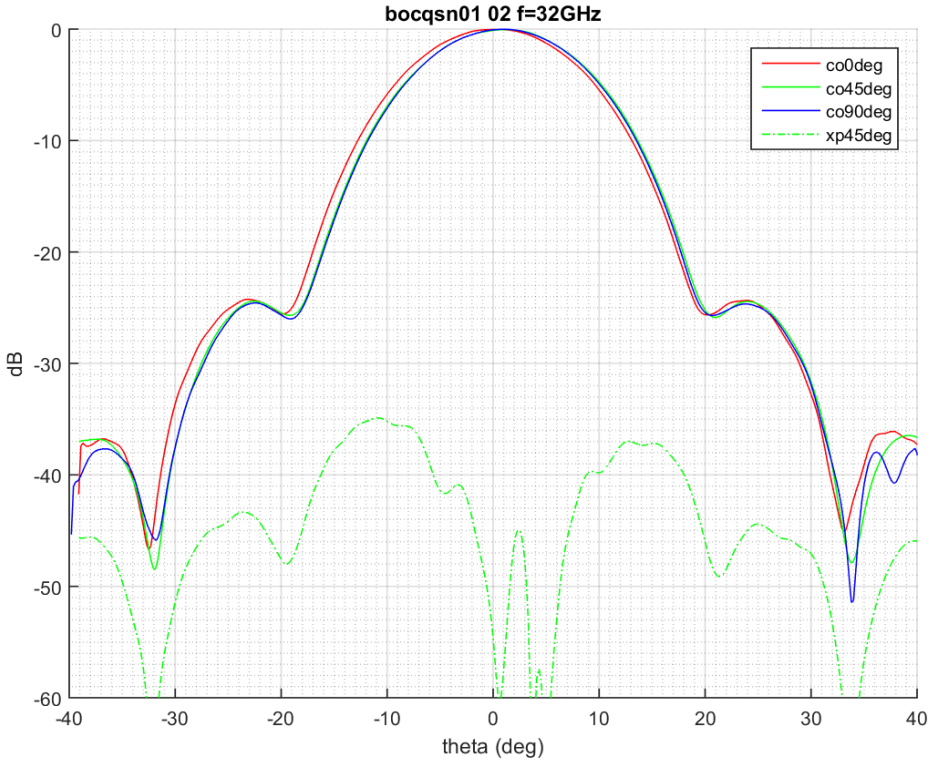

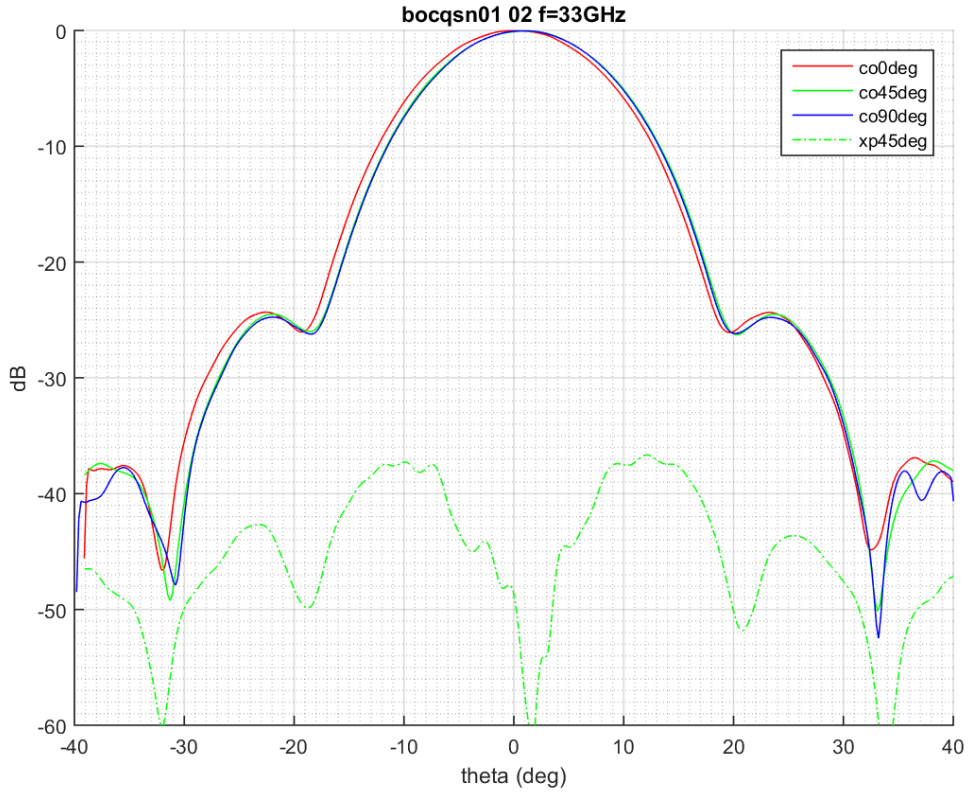
bocqsn01 02 f=33GHz
co0deg
co45deg
co90deg
xp45deg
dB
theta (deg)
0
-10
-20
-30
-40
-50
-60
-40
-30
-20
-10
0
10
20
30
40

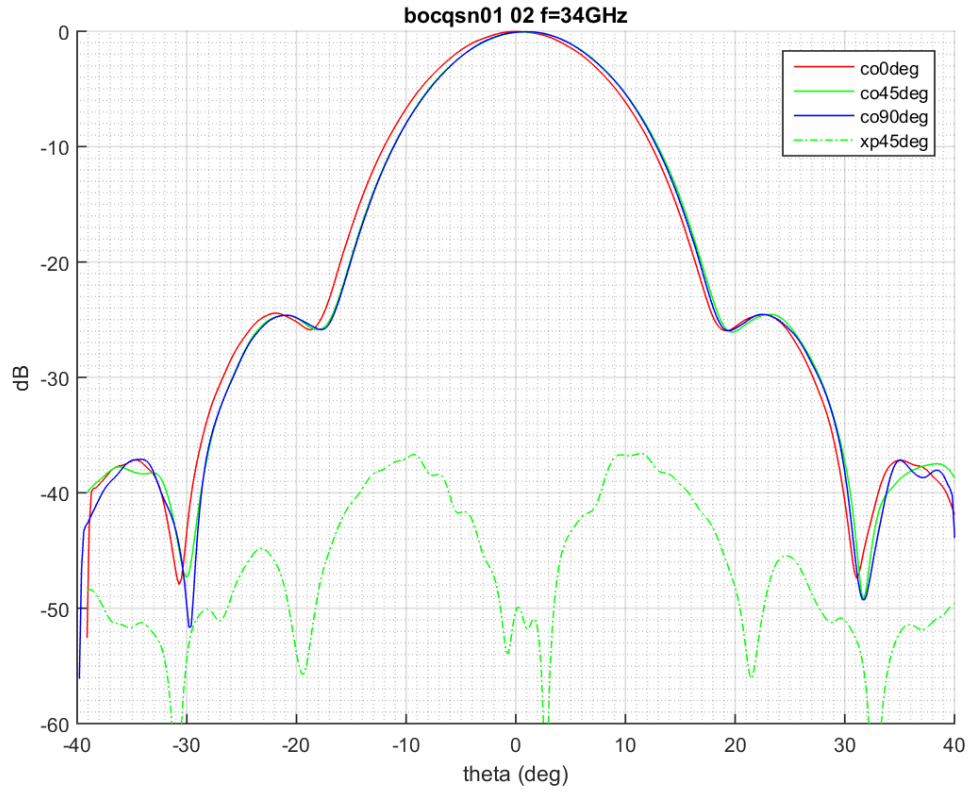
bocqsn01 02 f=34GHz
co0deg
co45deg
co90deg
xp45deg
dB
theta (deg)
0
-10
-20
-30
-40
-50
-60
-40
-30
-20
-10
0
10
20
30
40

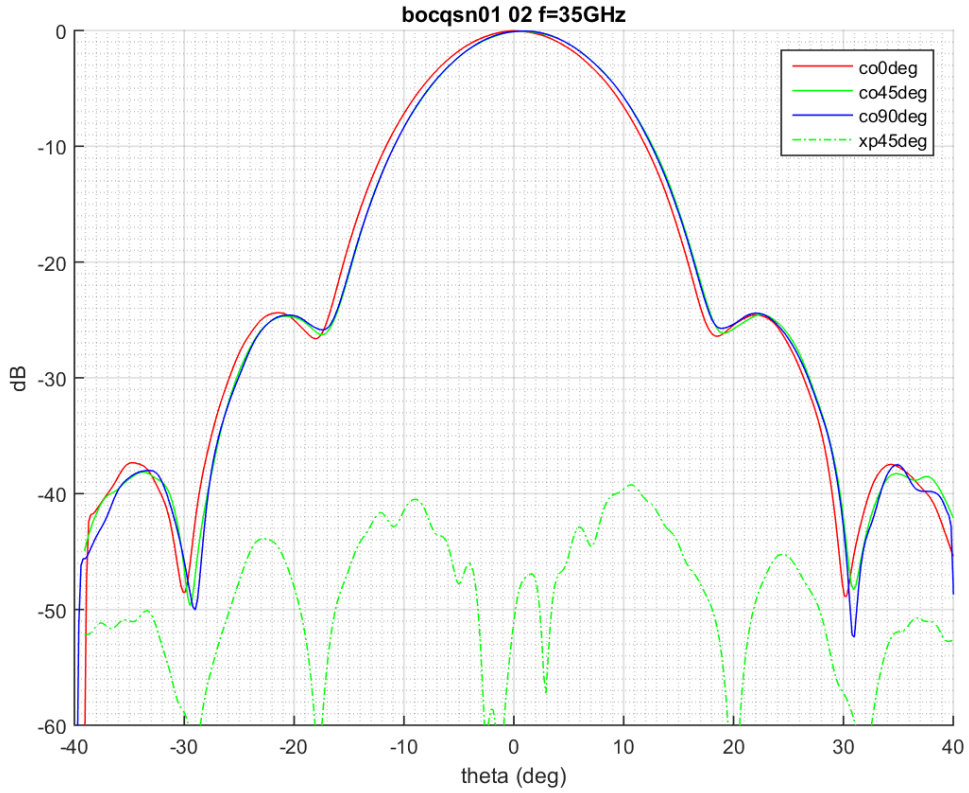
bocqsn01 02 f=35GHz
co0deg
co45deg
co90deg
xp45deg
dB
theta (deg)
0
-10
-20
-30
-40
-50
-60
-40
-30
-20
-10
0
10
20
30
40

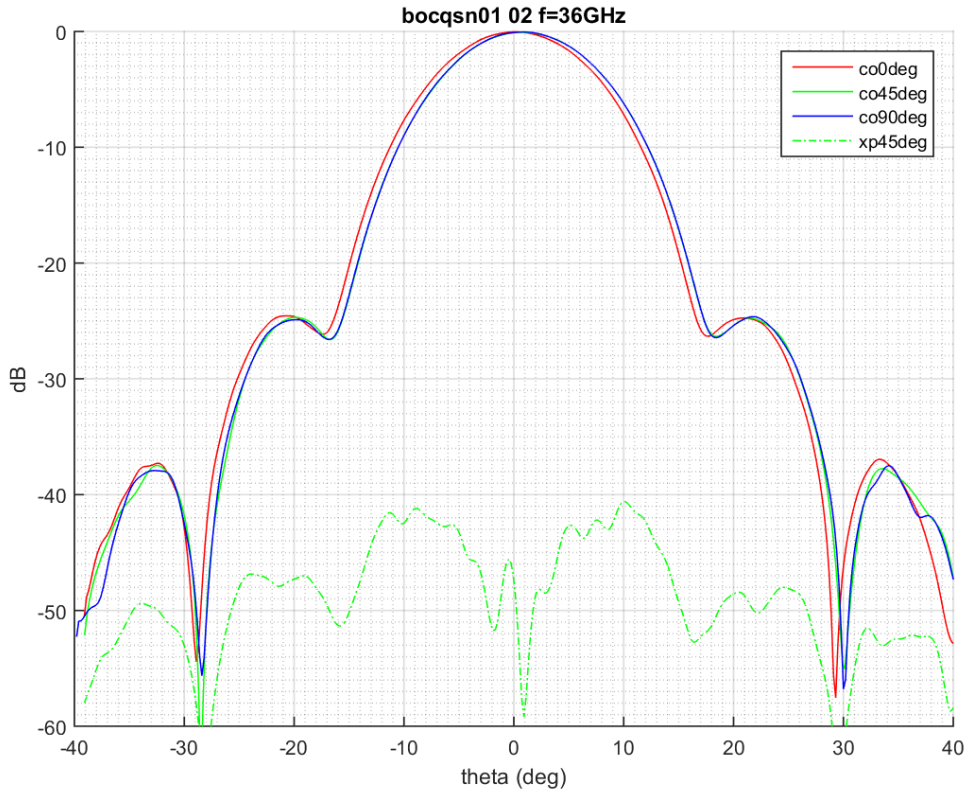
bocqsn01 02 f=36GHz
co0deg
co45deg
co90deg
xp45deg
dB
theta (deg)
0
-10
-20
-30
-40
-50
-60
-40
-30
-20
-10
0
10
20
30
40

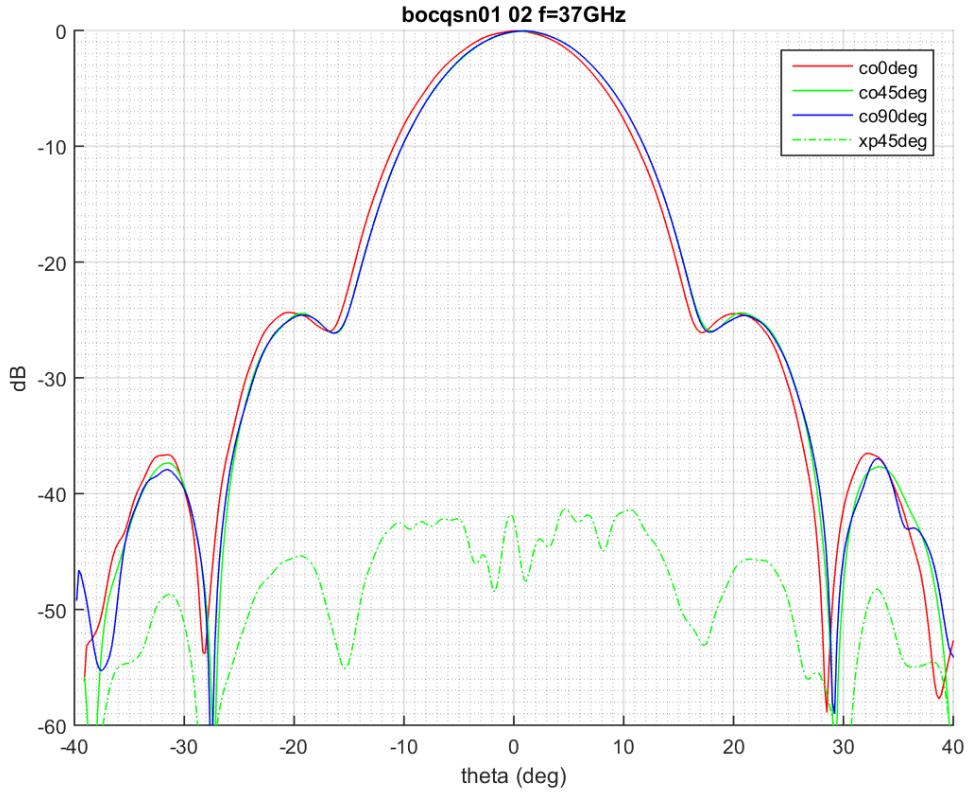
bocqsn01 02 f=37GHz
co0deg
co45deg
co90deg
xp45deg
dB
theta (deg)
0
-10
-20
-30
-40
-50
-60
-40
-30
-20
-10
0
10
20
30
40

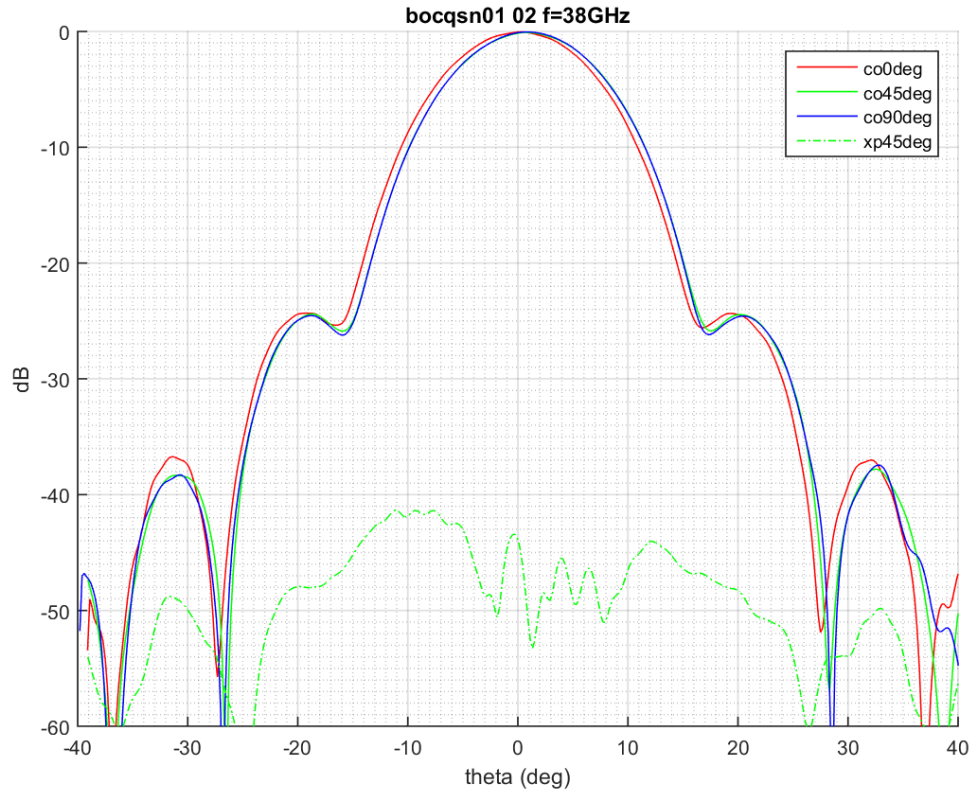
bocqsn01 02 f=38GHz
co0deg
co45deg
co90deg
xp45deg
dB
theta (deg)
0
-10
-20
-30
-40
-50
-60
-40
-30
-20
-10
0
10
20
30
40

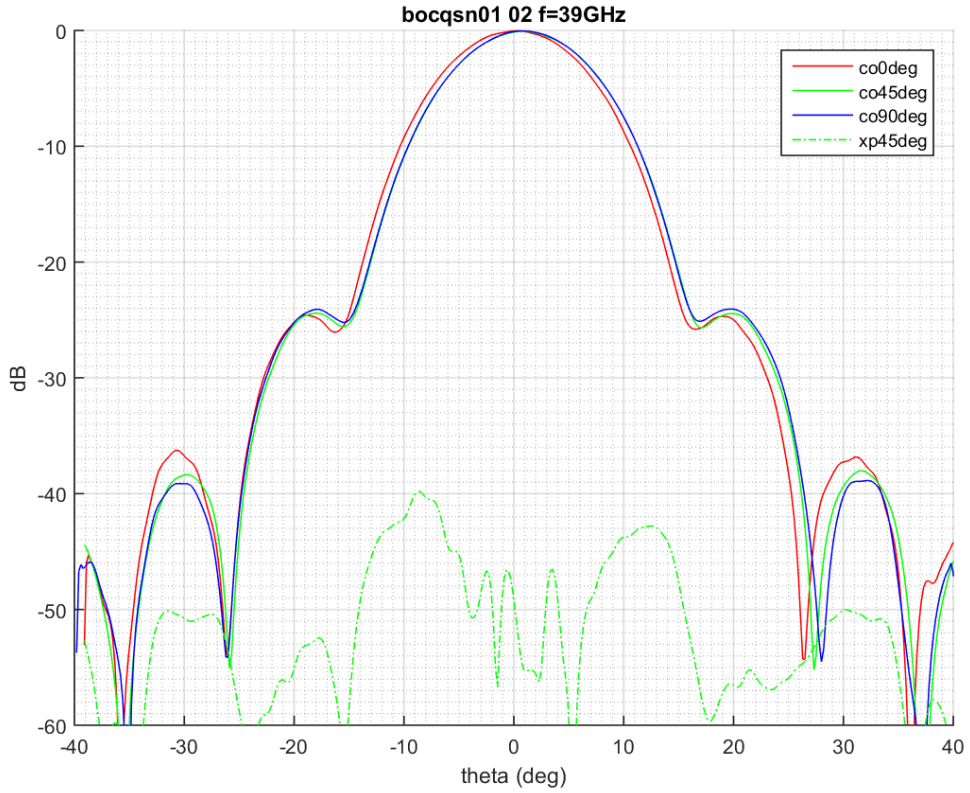
bocqsn01 02 f=39GHz
co0deg
co45deg
co90deg
xp45deg
dB
theta (deg)
0
-10
-20
-30
-40
-50
-60
-40
-30
-20
-10
0
10
20
30
40

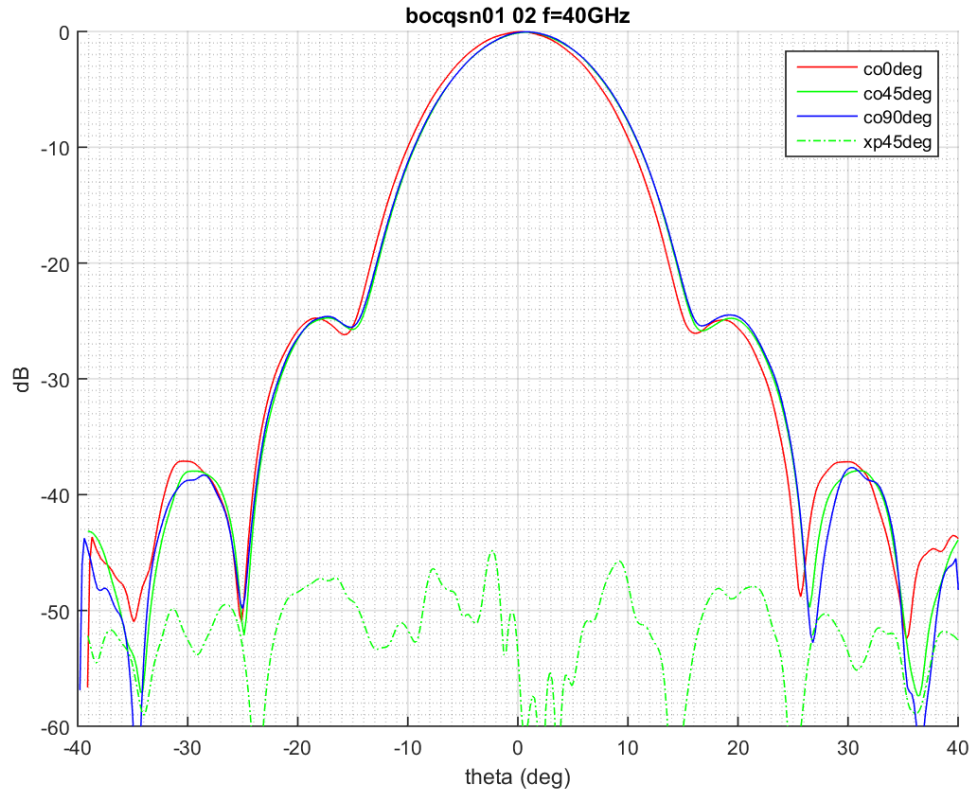
bocqsn01 02 f=40GHz
co0deg
co45deg
co90deg
xp45deg
dB
theta (deg)
0
-10
-20
-30
-40
-50
-60
-40
-30
-20
-10
0
10
20
30
40

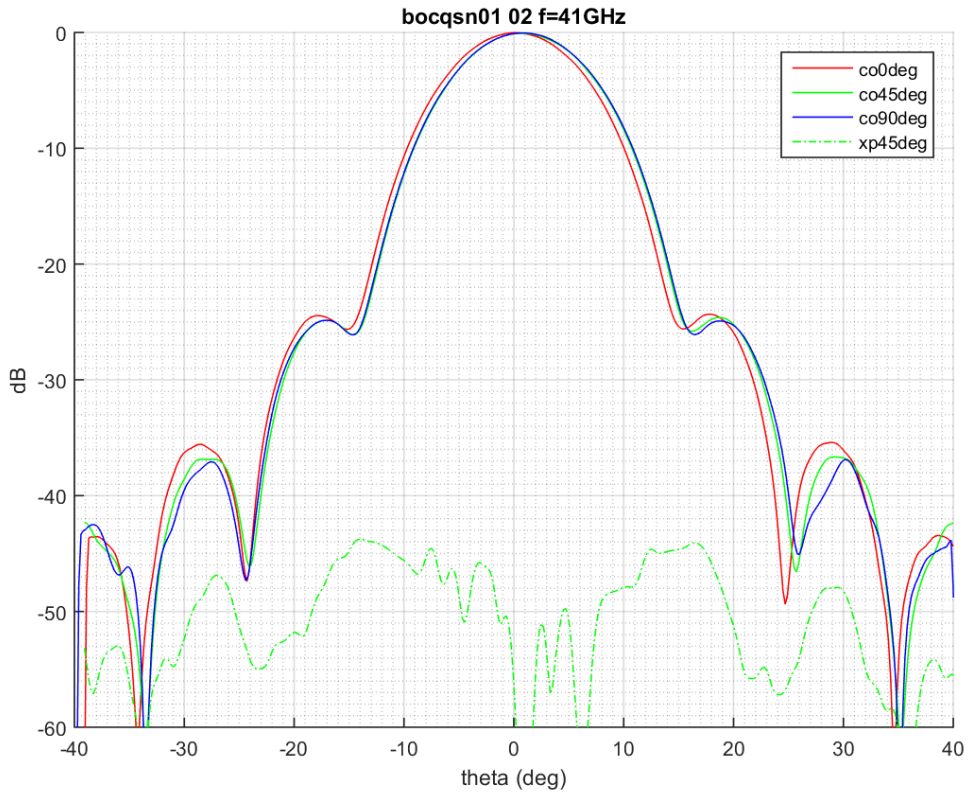
bocqsn01 02 f=41GHz
co0deg
co45deg
co90deg
xp45deg
dB
theta (deg)
0
-10
-20
-30
-40
-50
-60
-40
-30
-20
-10
0
10
20
30
40

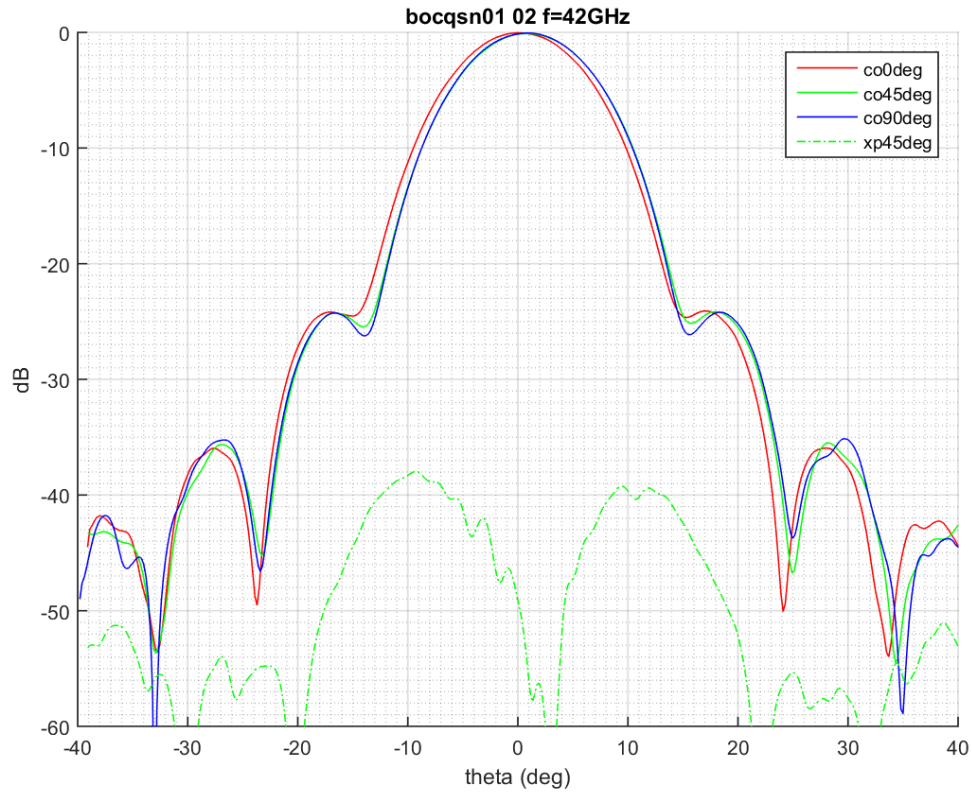
bocqsn01 02 f=42GHz
co0deg
co45deg
co90deg
xp45deg
dB
theta (deg)
0
-10
-20
-30
-40
-50
-60
-40
-30
-20
-10
0
10
20
30
40

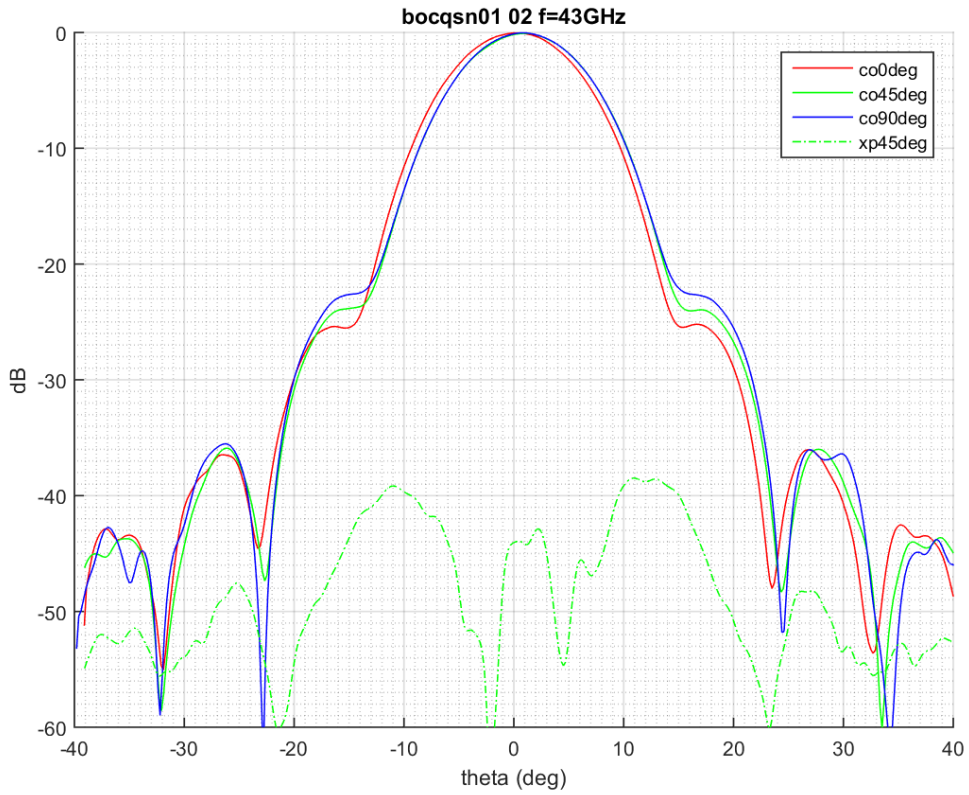
bocqsn01 02 f=43GHz
co0deg
co45deg
co90deg
xp45deg
dB
theta (deg)
0
-10
-20
-30
-40
-50
-60
-40
-30
-20
-10
0
10
20
30
40

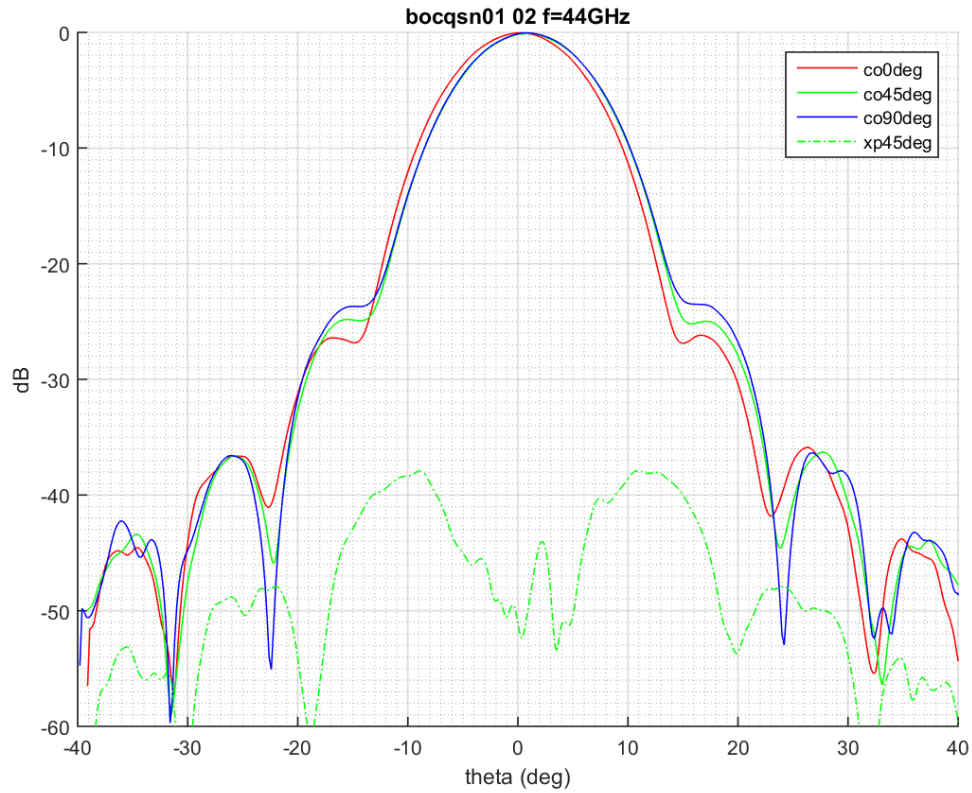
bocqsn01 02 f=44GHz
co0deg
co45deg
co90deg
xp45deg
dB
theta (deg)
0
-10
-20
-30
-40
-50
-60
-40
-30
-20
-10
0
10
20
30
40

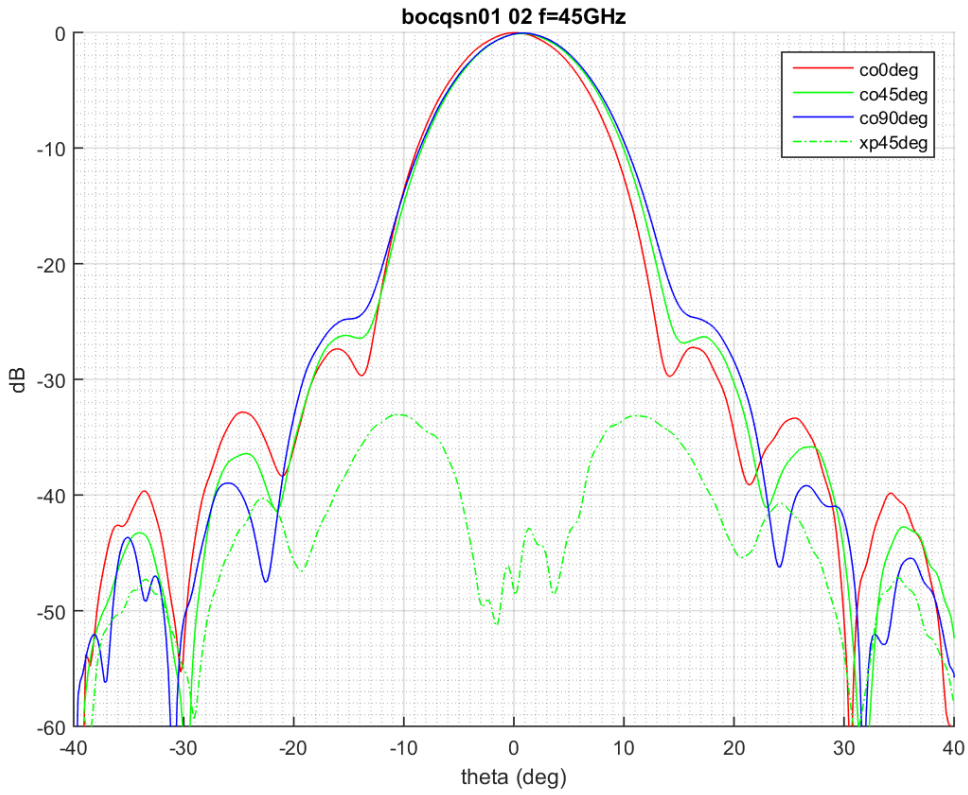
bocqsn01 02 f=45GHz
co0deg
co45deg
co90deg
xp45deg
dB
theta (deg)
0
-10
-20
-30
-40
-50
-60
-40
-30
-20
-10
0
10
20
30
40

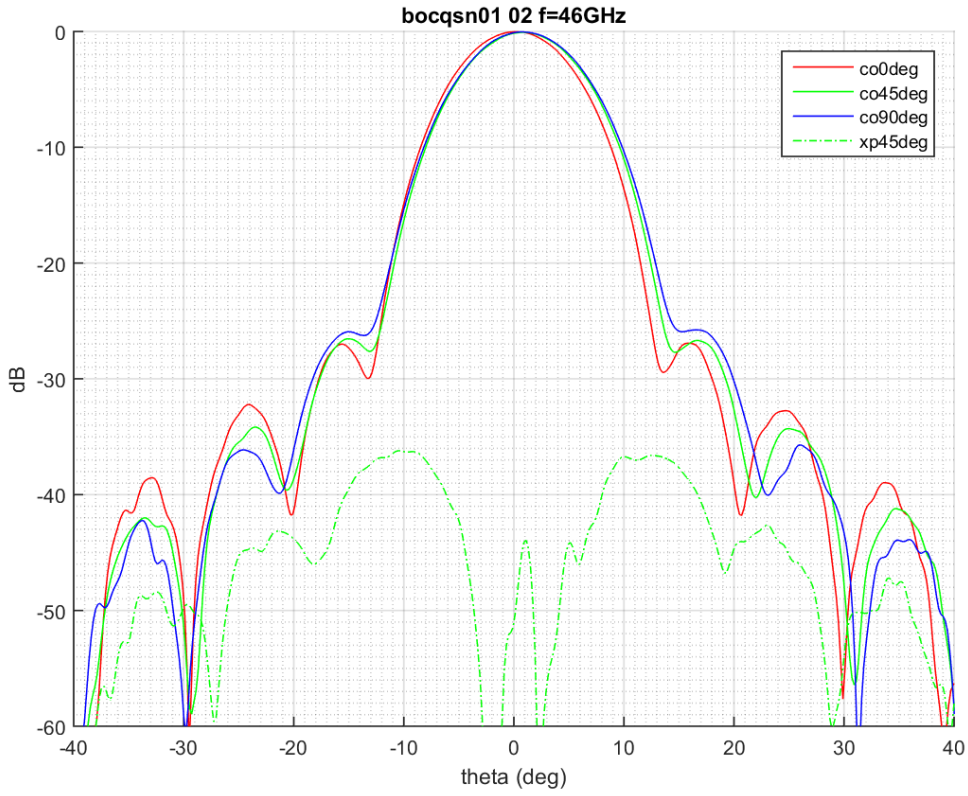
bocqsn01 02 f=46GHz
co0deg
co45deg
co90deg
xp45deg
dB
theta (deg)
0
-10
-20
-30
-40
-50
-60
-40
-30
-20
-10
0
10
20
30
40

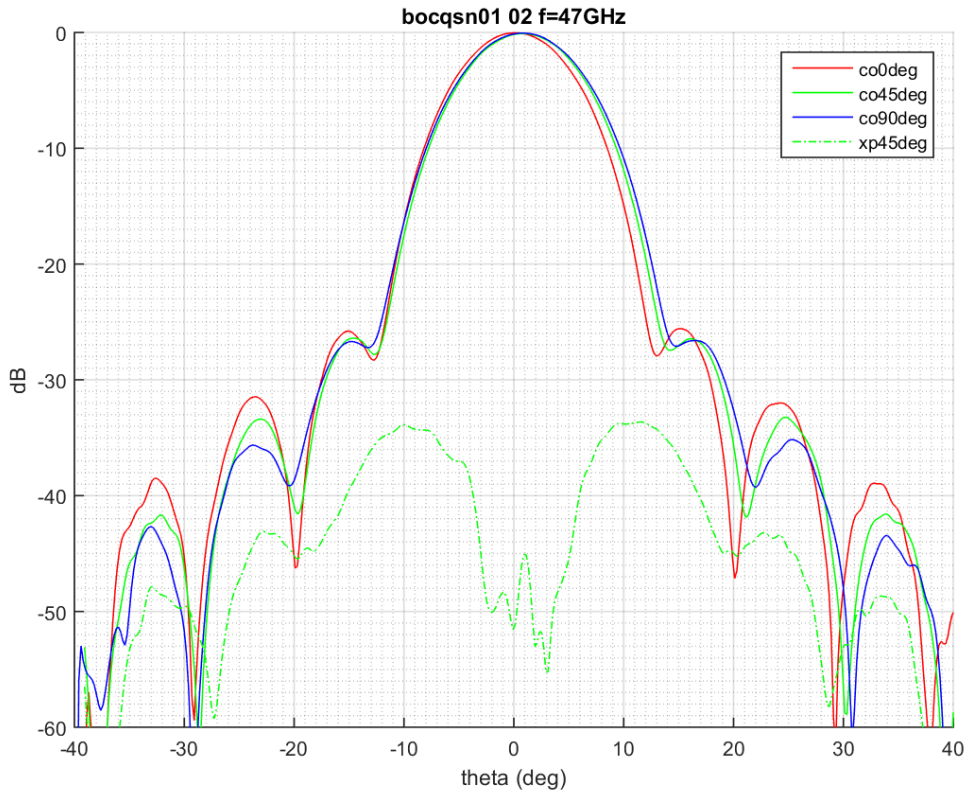
bocqsn01 02 f=47GHz
co0deg
co45deg
co90deg
xp45deg
dB
theta (deg)
0
-10
-20
-30
-40
-50
-60
-40
-30
-20
-10
0
10
20
30
40

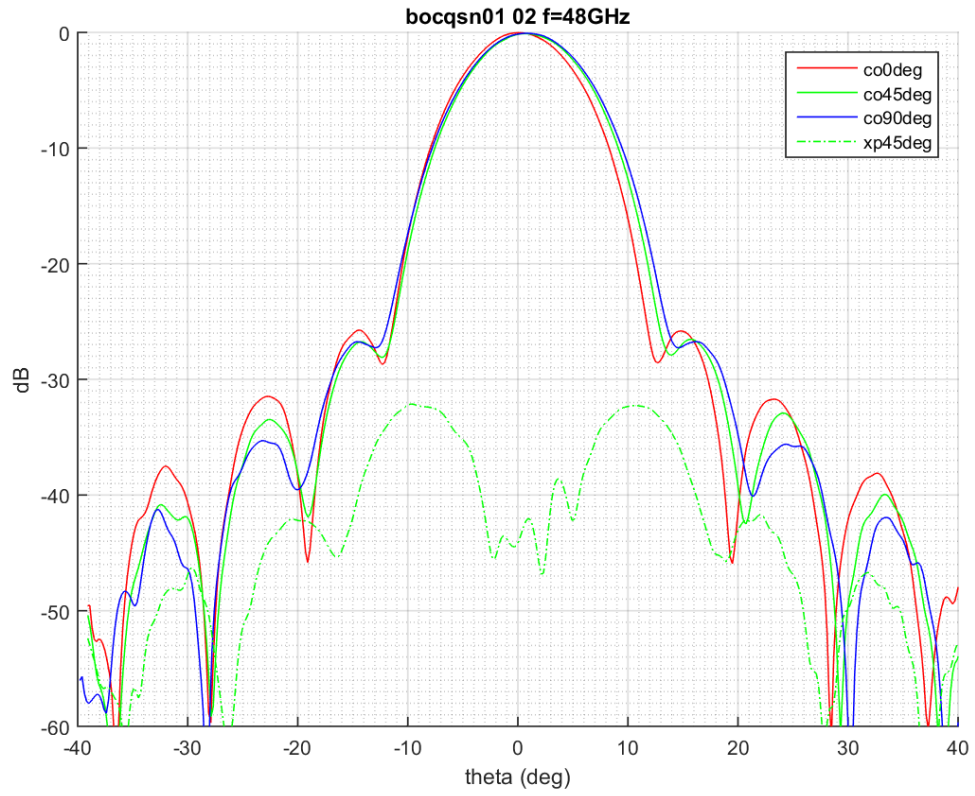
bocqsn01 02 f=48GHz
co0deg
co45deg
co90deg
xp45deg
dB
theta (deg)
0
-10
-20
-30
-40
-50
-60
-40
-30
-20
-10
0
10
20
30
40

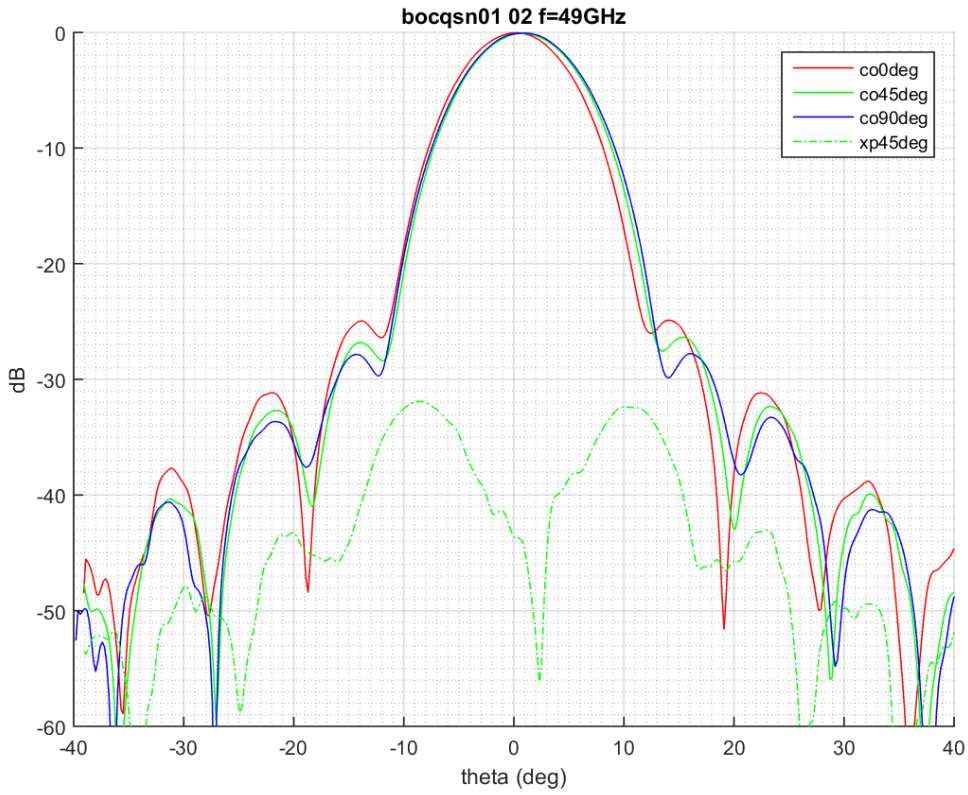
bocqsn01 02 f=49GHz
co0deg
co45deg
co90deg
xp45deg
dB
theta (deg)
0
-10
-20
-30
-40
-50
-60
-40
-30
-20
-10
0
10
20
30
40

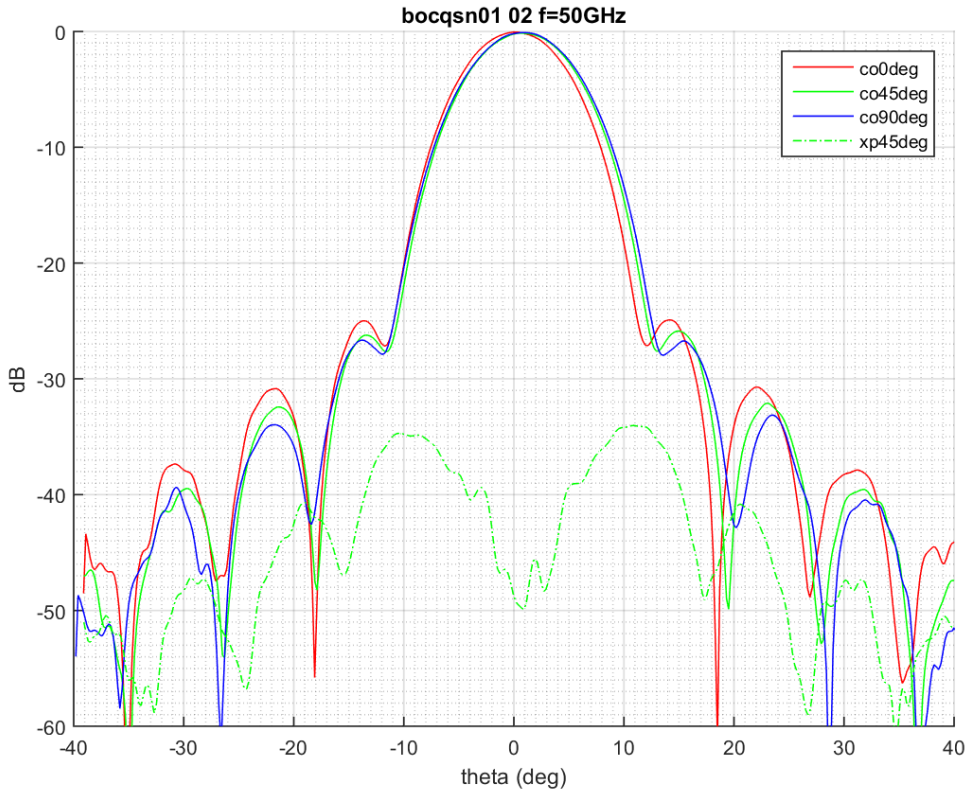
bocqsn01 02 f=50GHz
co0deg
co45deg
co90deg
xp45deg
dB
theta (deg)
0
-10
-20
-30
-40
-50
-60
-40
-30
-20
-10
0
10
20
30
40

Appendix D. Q-band radiation patterns sn02

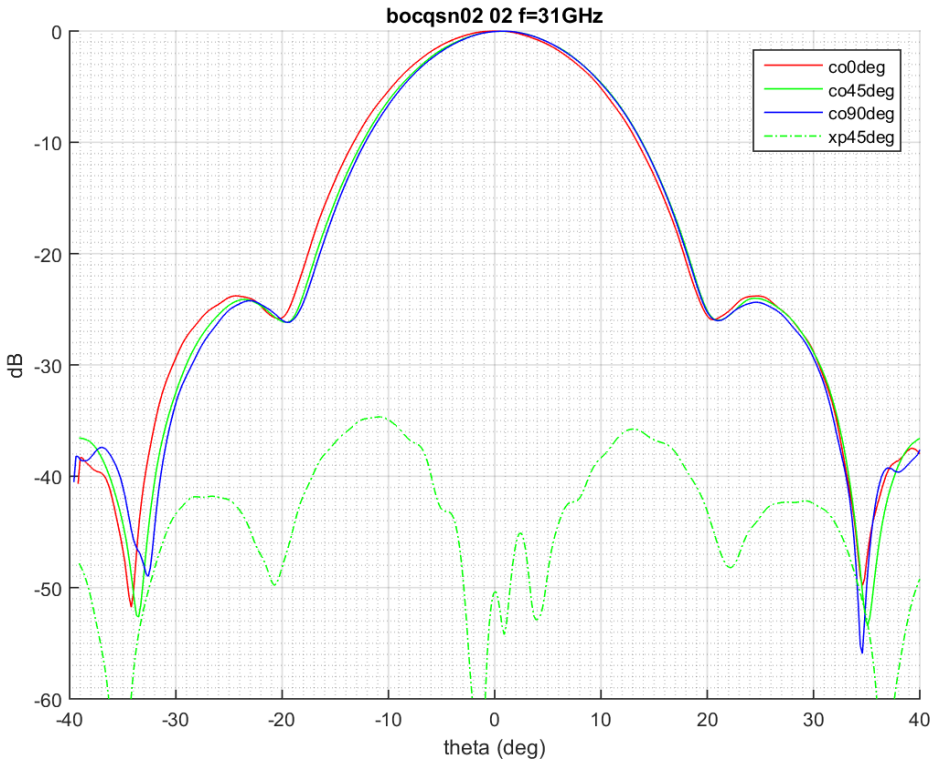

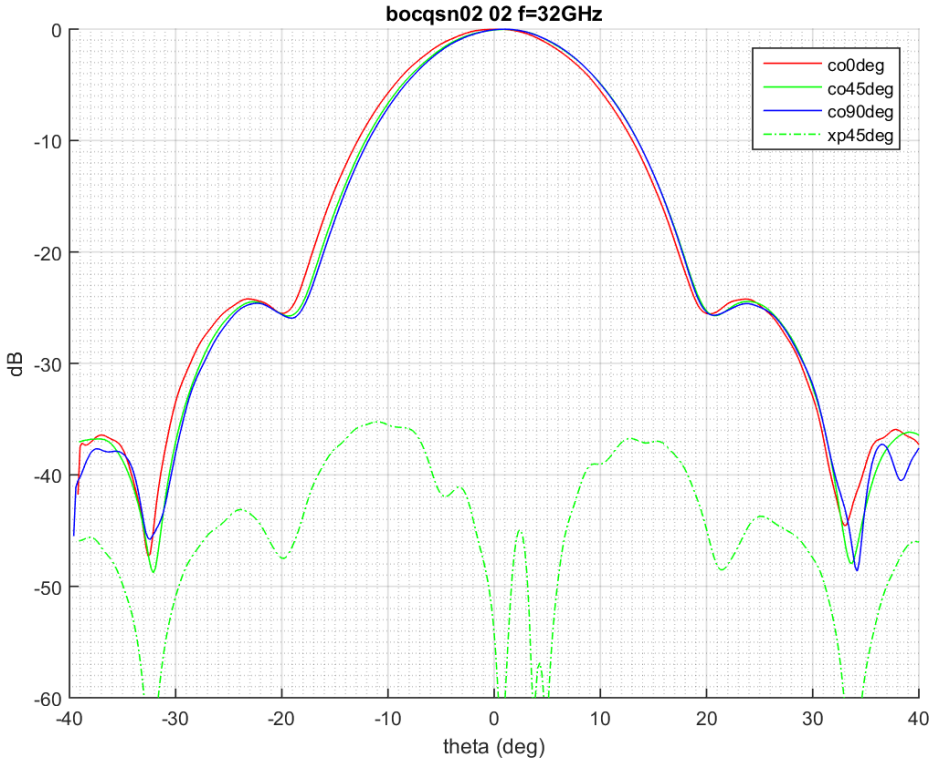

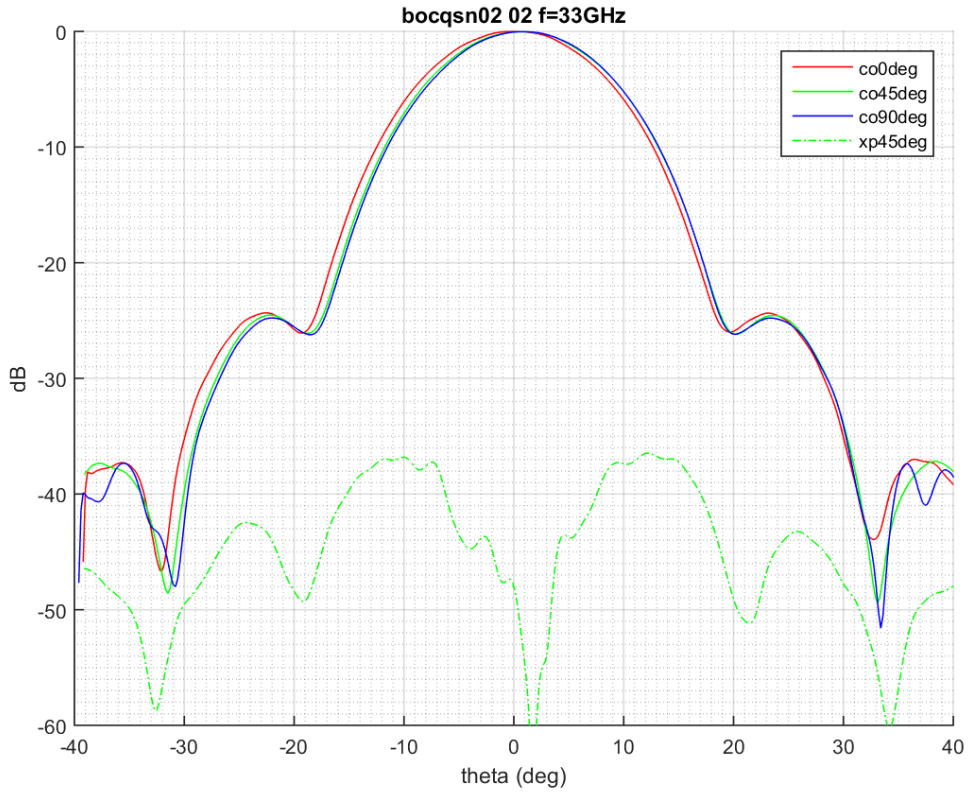
bocqsn02 02 f=33GHz
co0deg
co45deg
co90deg
xp45deg
dB
theta (deg)
0
-10
-20
-30
-40
-50
-60
-40
-30
-20
-10
0
10
20
30
40

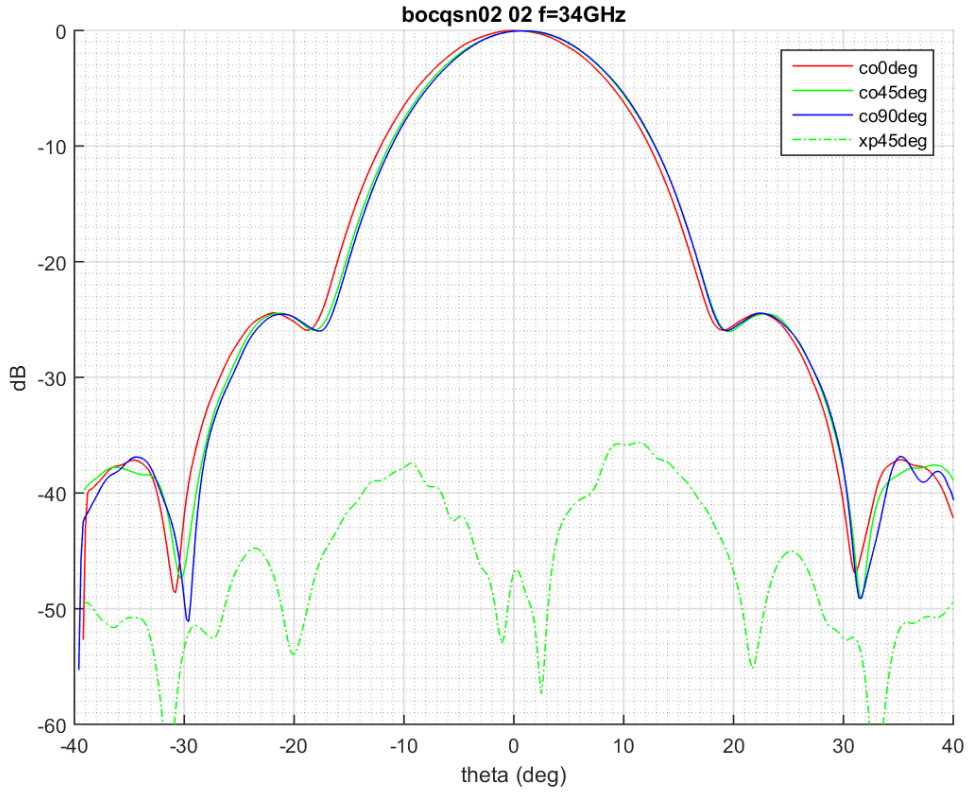
bocqsn02 02 f=34GHz
co0deg
co45deg
co90deg
xp45deg
dB
theta (deg)
0
-10
-20
-30
-40
-50
-60
-40
-30
-20
-10
0
10
20
30
40

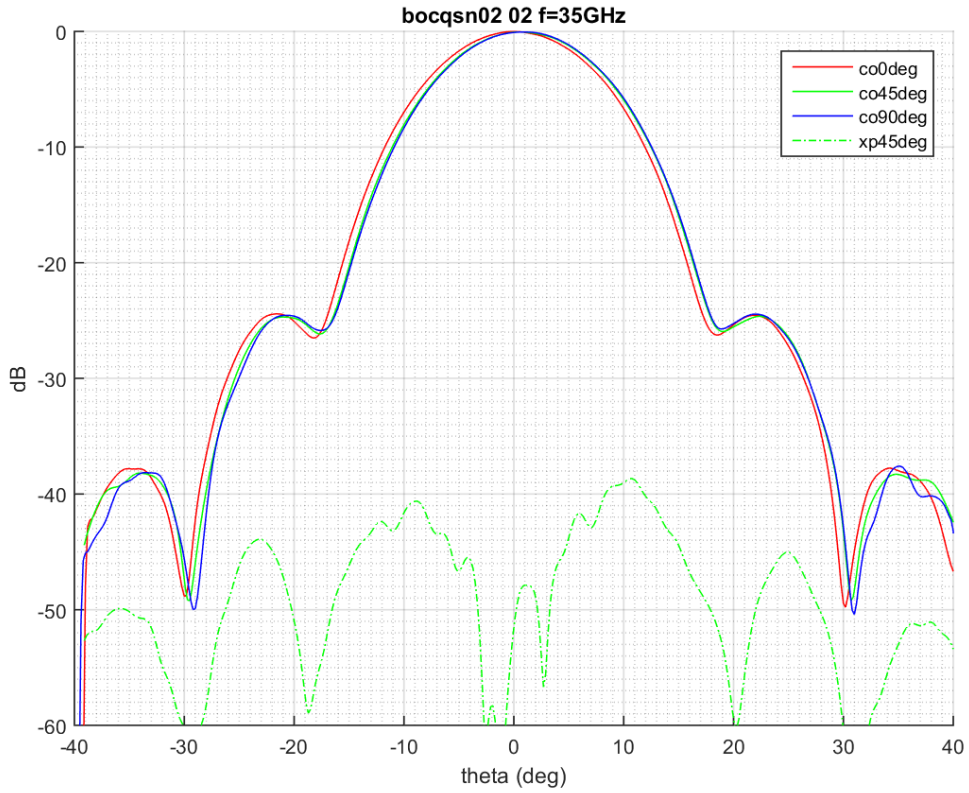
bocqsn02 02 f=35GHz
co0deg
co45deg
co90deg
xp45deg
dB
theta (deg)
0
-10
-20
-30
-40
-50
-60
-40
-30
-20
-10
0
10
20
30
40

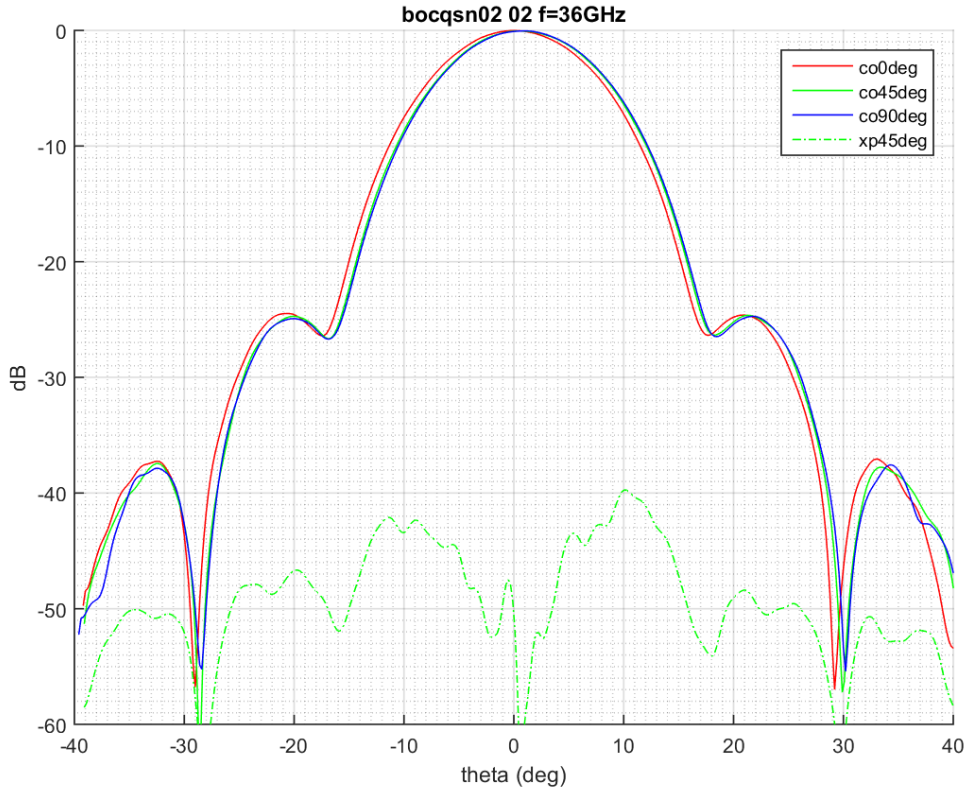
bocqsn02 02 f=36GHz
co0deg
co45deg
co90deg
xp45deg
dB
theta (deg)
0
-10
-20
-30
-40
-50
-60
-40
-30
-20
-10
0
10
20
30
40

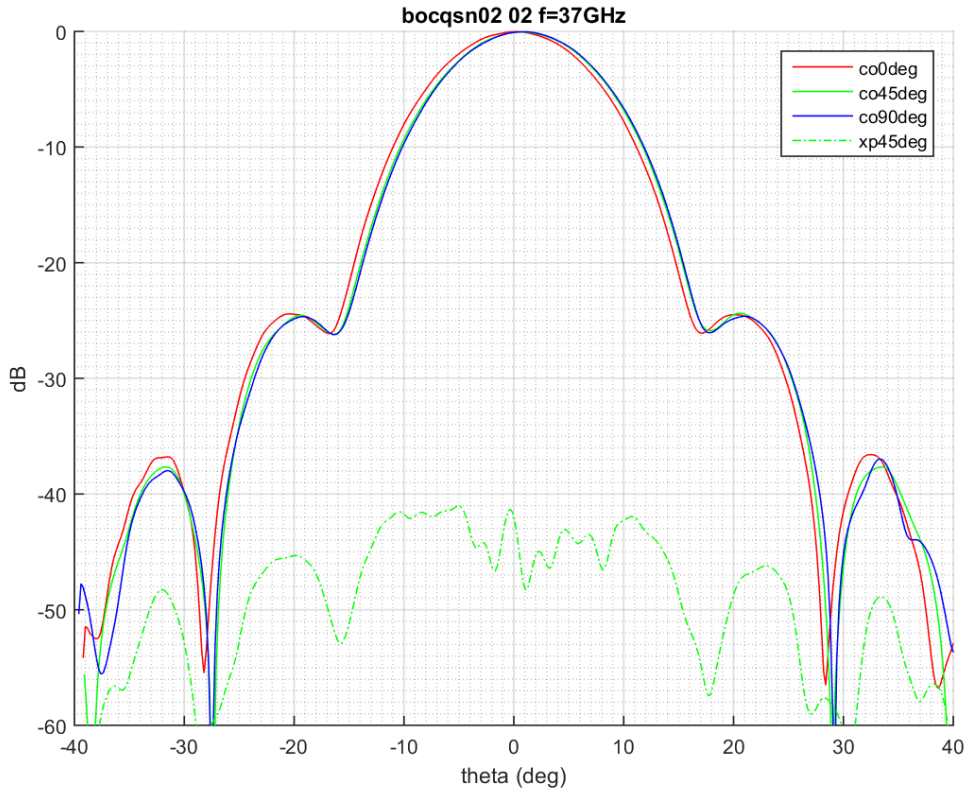
bocqsn02 02 f=37GHz
co0deg
co45deg
co90deg
xp45deg
dB
theta (deg)
0
-10
-20
-30
-40
-50
-60
-40
-30
-20
-10
0
10
20
30
40

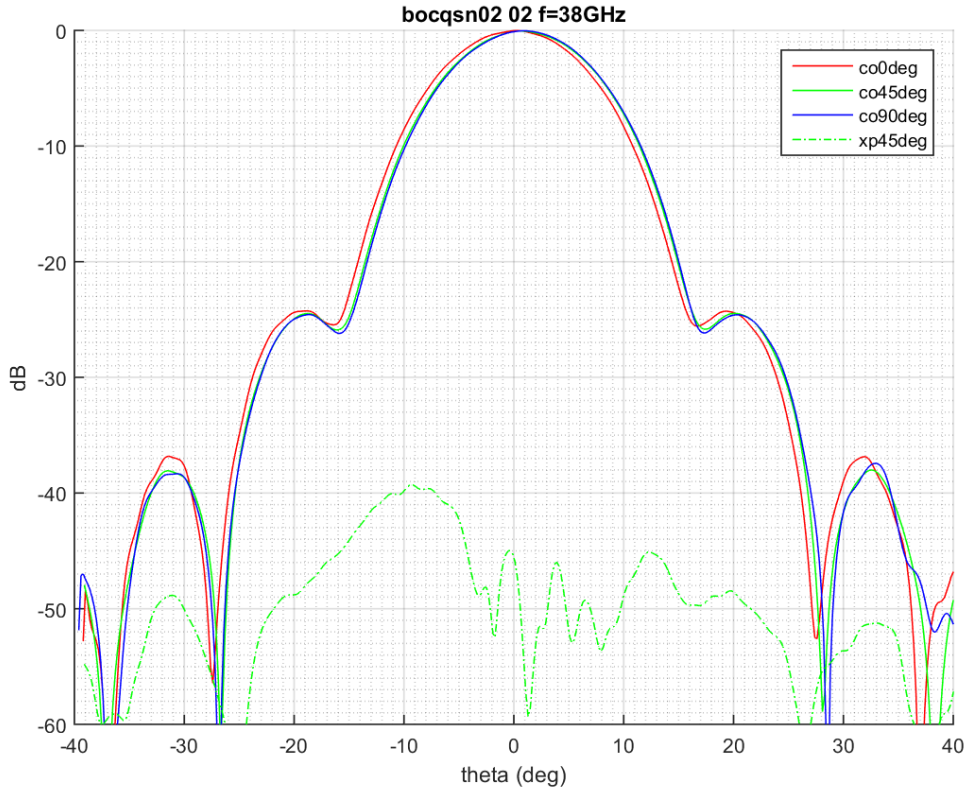
bocqsn02 02 f=38GHz
co0deg
co45deg
co90deg
xp45deg
dB
theta (deg)
0
-10
-20
-30
-40
-50
-60
-40
-30
-20
-10
0
10
20
30
40

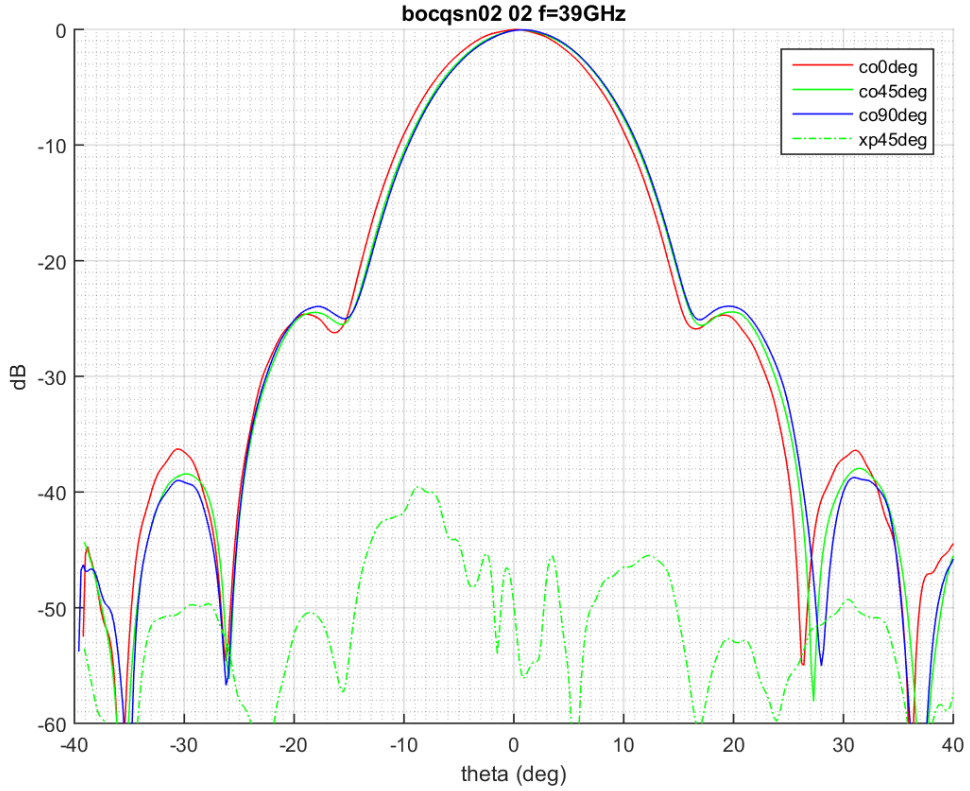
bocqsn02 02 f=39GHz
co0deg
co45deg
co90deg
xp45deg
dB
theta (deg)
0
-10
-20
-30
-40
-50
-60
-40
-30
-20
-10
0
10
20
30
40

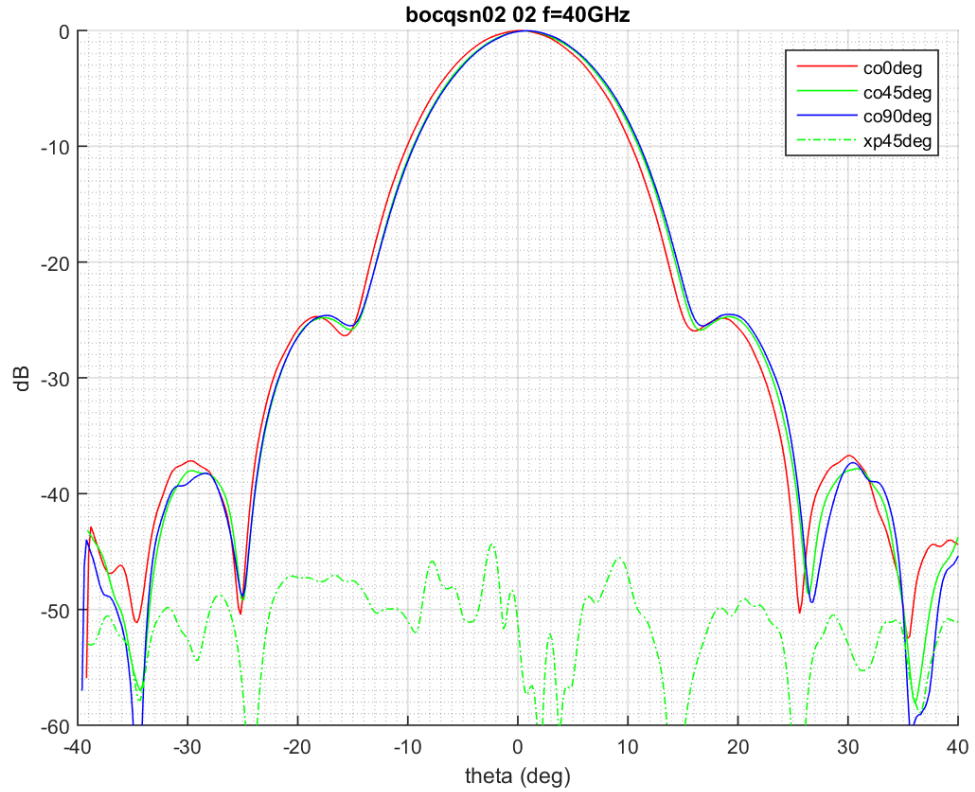
bocqsn02 02 f=40GHz
co0deg
co45deg
co90deg
xp45deg
dB
theta (deg)
0
-10
-20
-30
-40
-50
-60
-40
-30
-20
-10
0
10
20
30
40

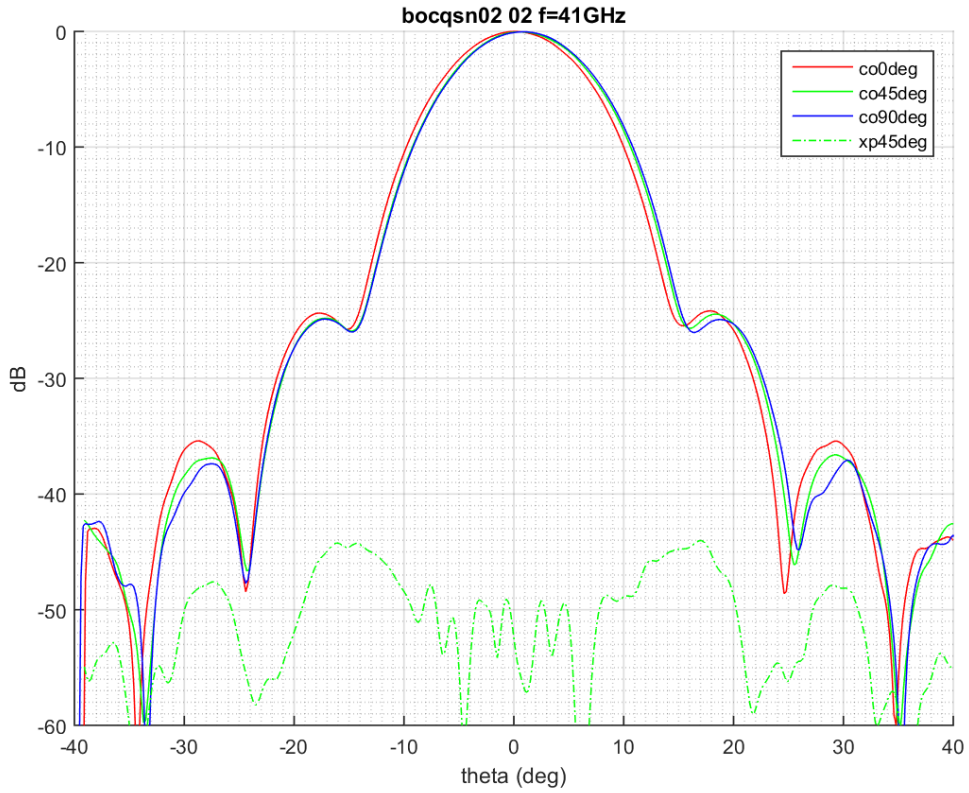
bocqsn02 02 f=41GHz
co0deg
co45deg
co90deg
xp45deg
dB
theta (deg)
0
-10
-20
-30
-40
-50
-60
-40
-30
-20
-10
0
10
20
30
40

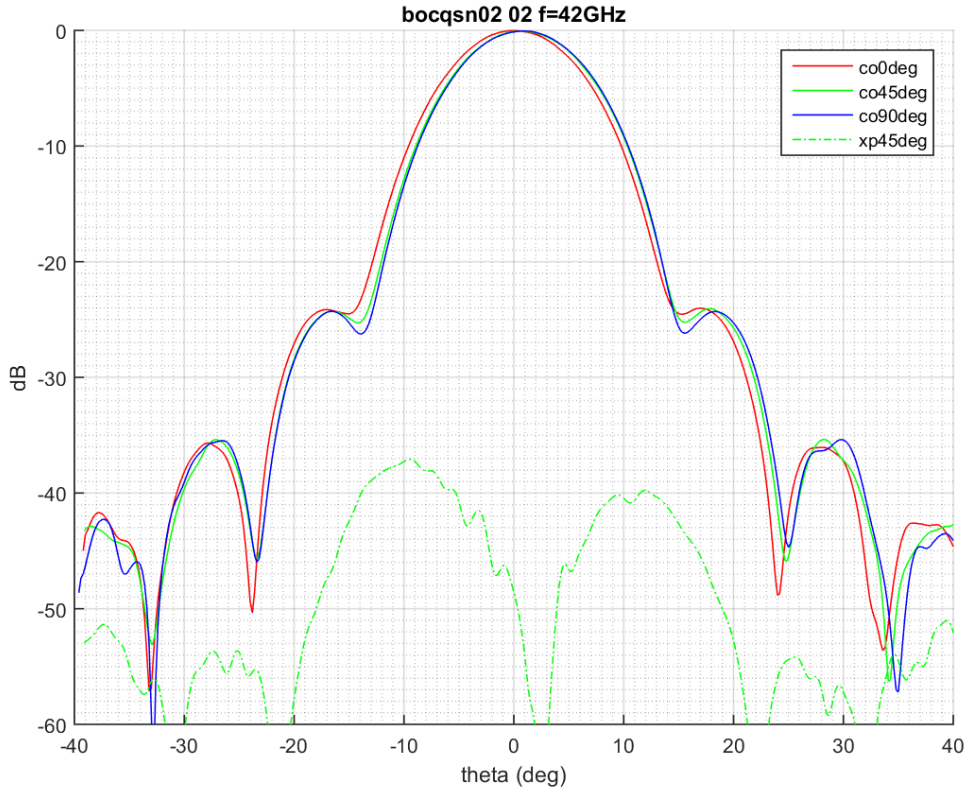
bocqsn02 02 f=42GHz
co0deg
co45deg
co90deg
xp45deg
dB
theta (deg)
0
-10
-20
-30
-40
-50
-60
-40
-30
-20
-10
0
10
20
30
40

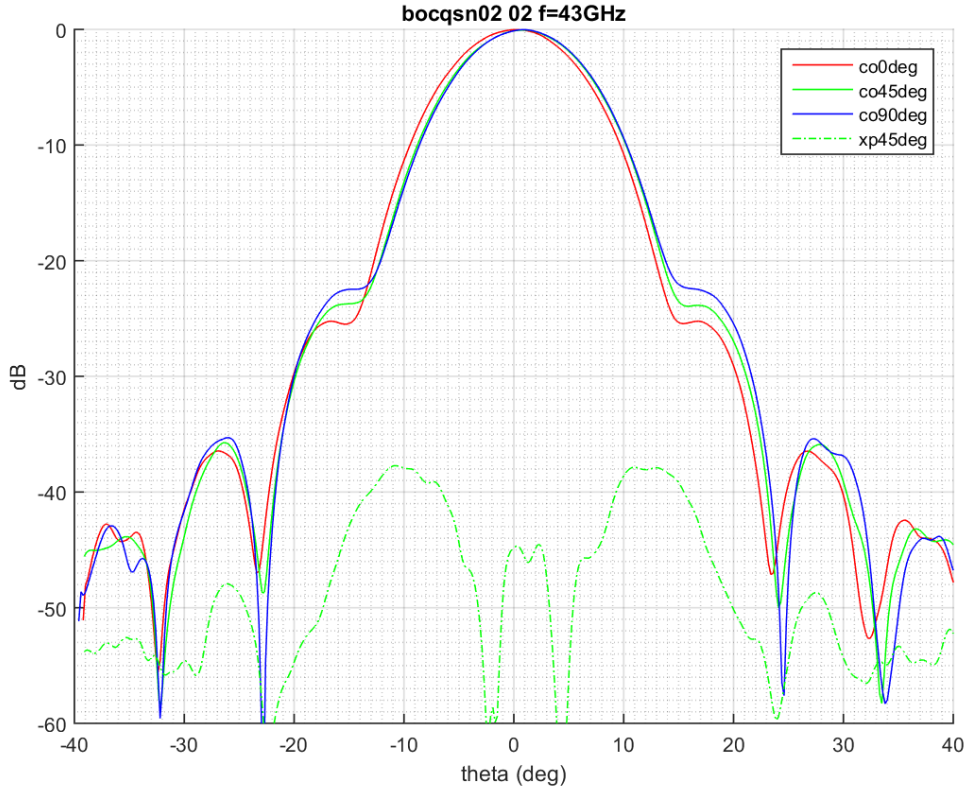
bocqsn02 02 f=43GHz
co0deg
co45deg
co90deg
xp45deg
dB
theta (deg)
0
-10
-20
-30
-40
-50
-60
-40
-30
-20
-10
0
10
20
30
40

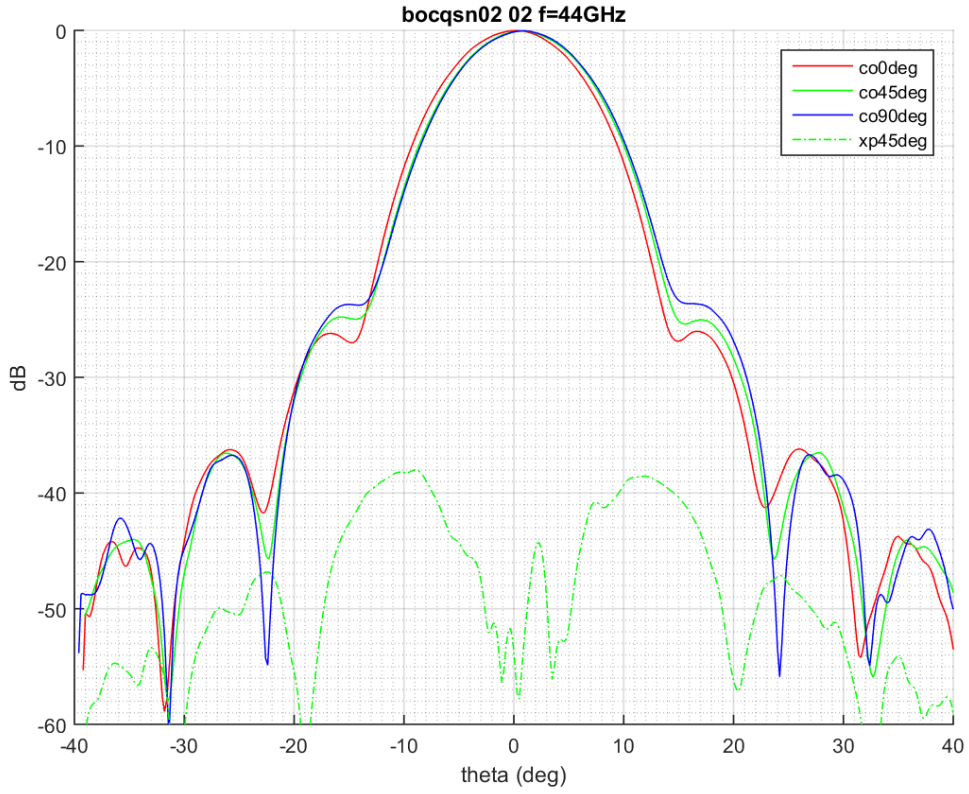
bocqsn02 02 f=44GHz
co0deg
co45deg
co90deg
xp45deg
dB
theta (deg)
0
-10
-20
-30
-40
-50
-60
-40
-30
-20
-10
0
10
20
30
40

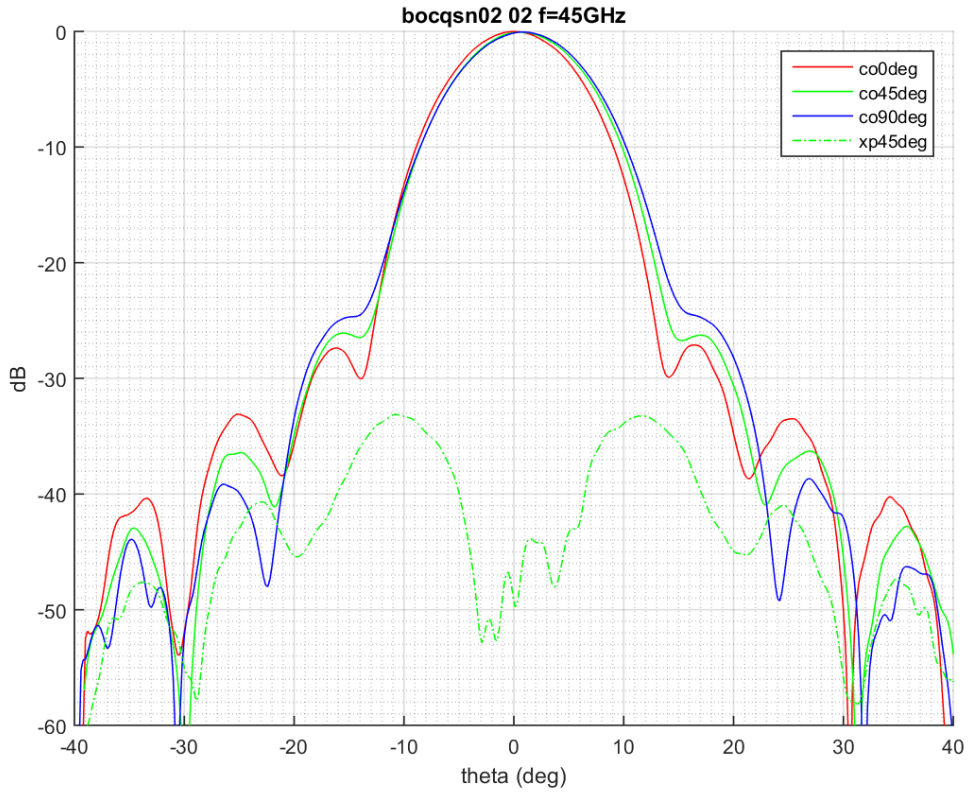
bocqsn02 02 f=45GHz
co0deg
co45deg
co90deg
xp45deg
dB
theta (deg)
0
-10
-20
-30
-40
-50
-60
-40
-30
-20
-10
0
10
20
30
40

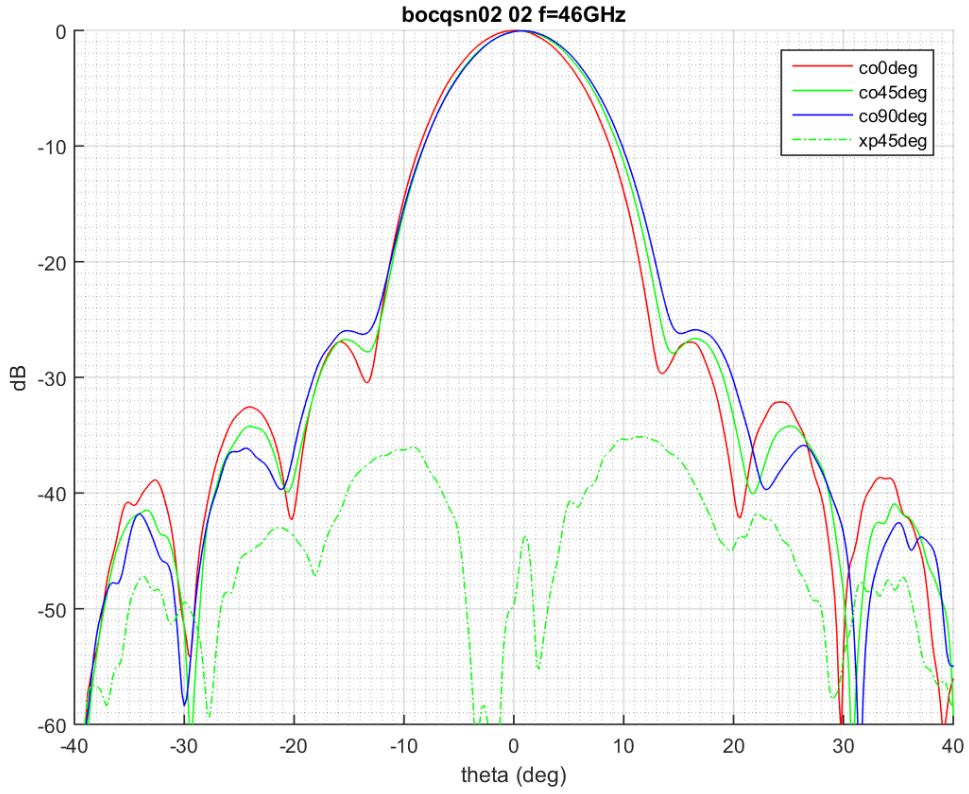
bocqsn02 02 f=46GHz
co0deg
co45deg
co90deg
xp45deg
dB
theta (deg)
0
-10
-20
-30
-40
-50
-60
-40
-30
-20
-10
0
10
20
30
40

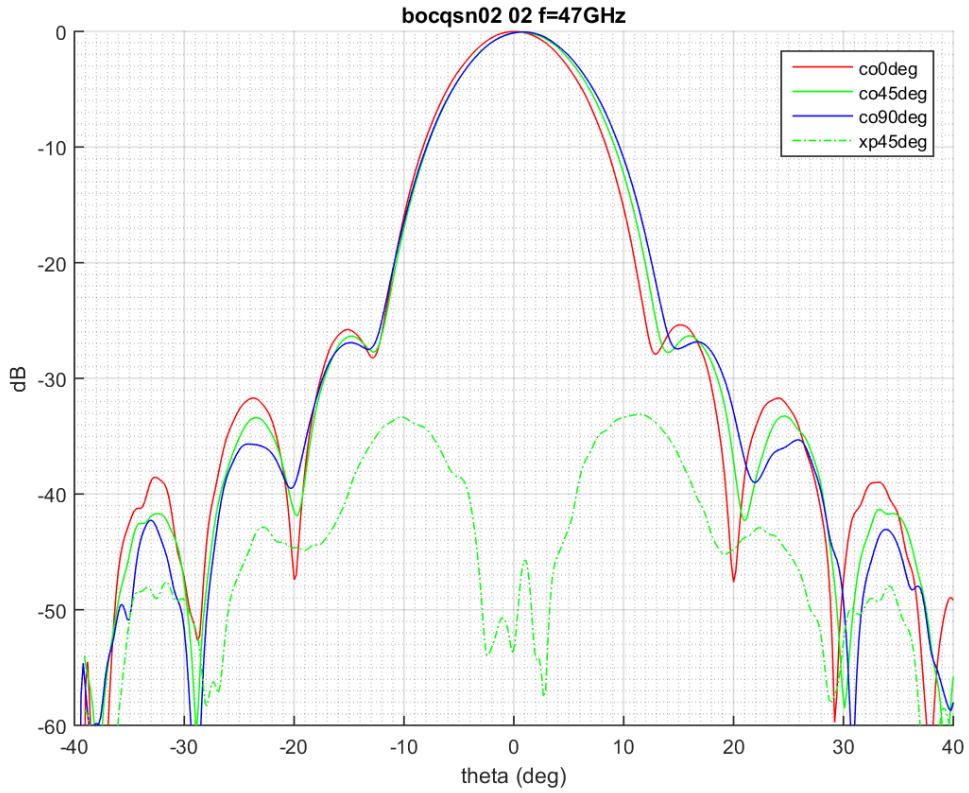
bocqsn02 02 f=47GHz
co0deg
co45deg
co90deg
xp45deg
dB
theta (deg)
0
-10
-20
-30
-40
-50
-60
-40
-30
-20
-10
0
10
20
30
40

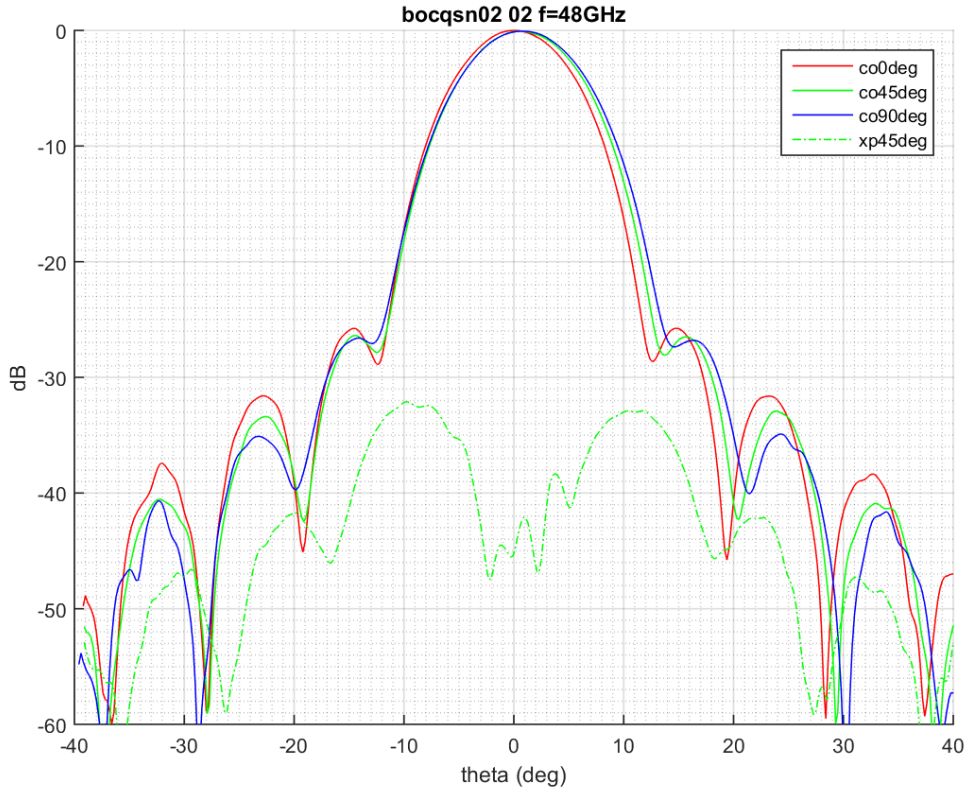
bocqsn02 02 f=48GHz
co0deg
co45deg
co90deg
xp45deg
dB
theta (deg)
0
-10
-20
-30
-40
-50
-60
-40
-30
-20
-10
0
10
20
30
40

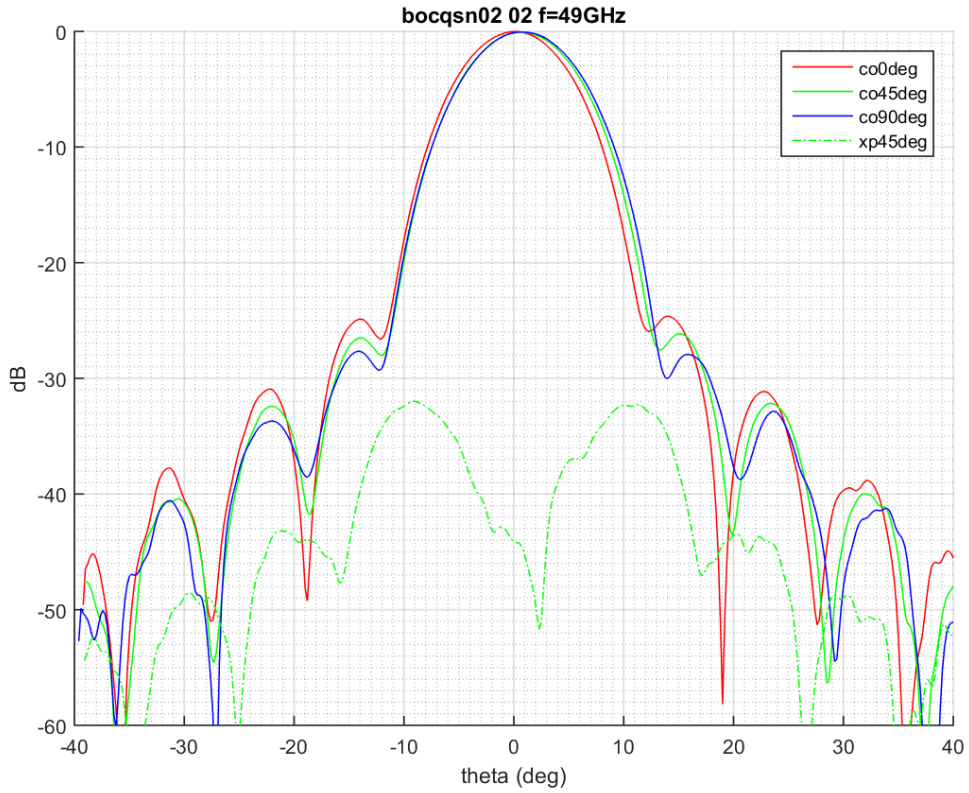
bocqsn02 02 f=49GHz
co0deg
co45deg
co90deg
xp45deg
dB
theta (deg)
0
-10
-20
-30
-40
-50
-60
-40
-30
-20
-10
0
10
20
30
40

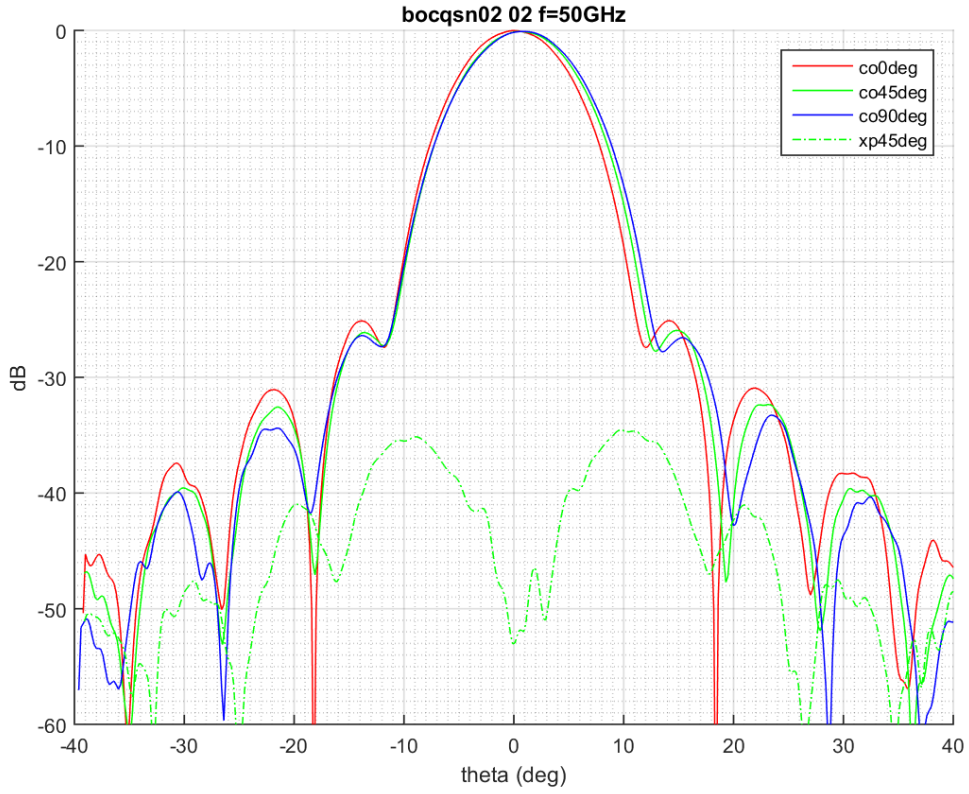
bocqsn02 02 f=50GHz
co0deg
co45deg
co90deg
xp45deg
dB
theta (deg)
0
-10
-20
-30
-40
-50
-60
-40
-30
-20
-10
0
10
20
30
40

Appendix E. W band radiation patterns sn01

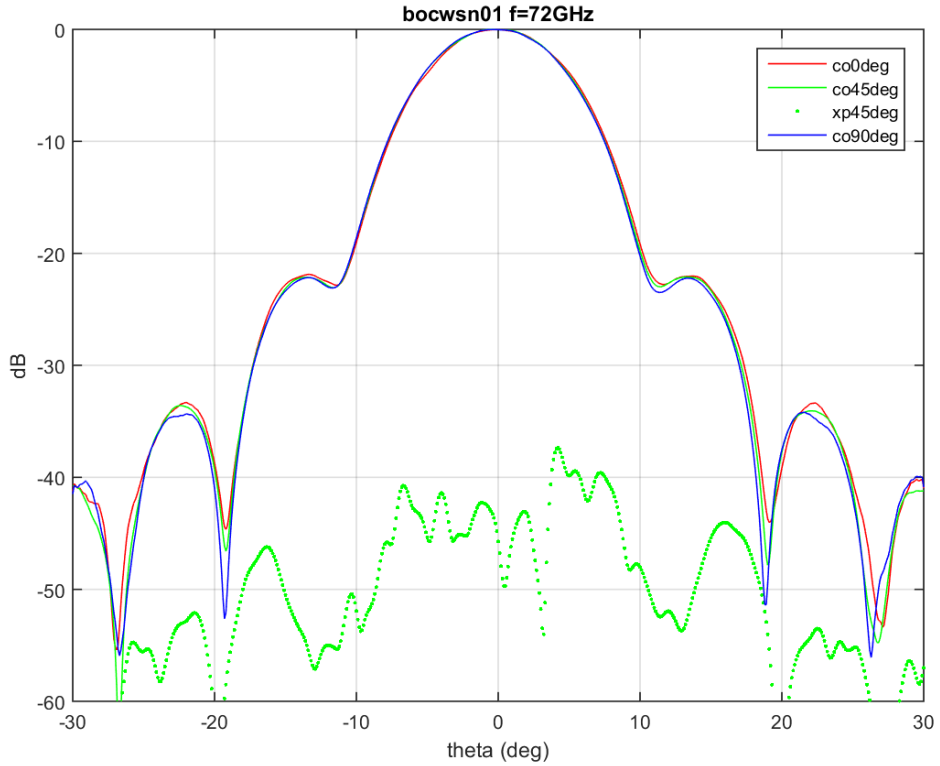

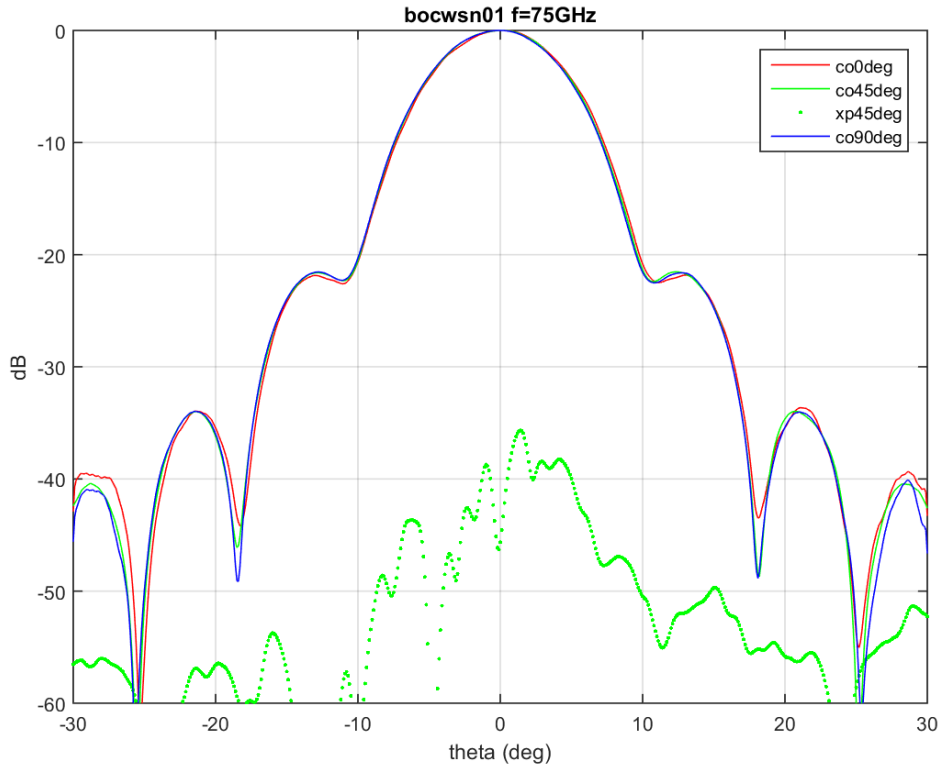

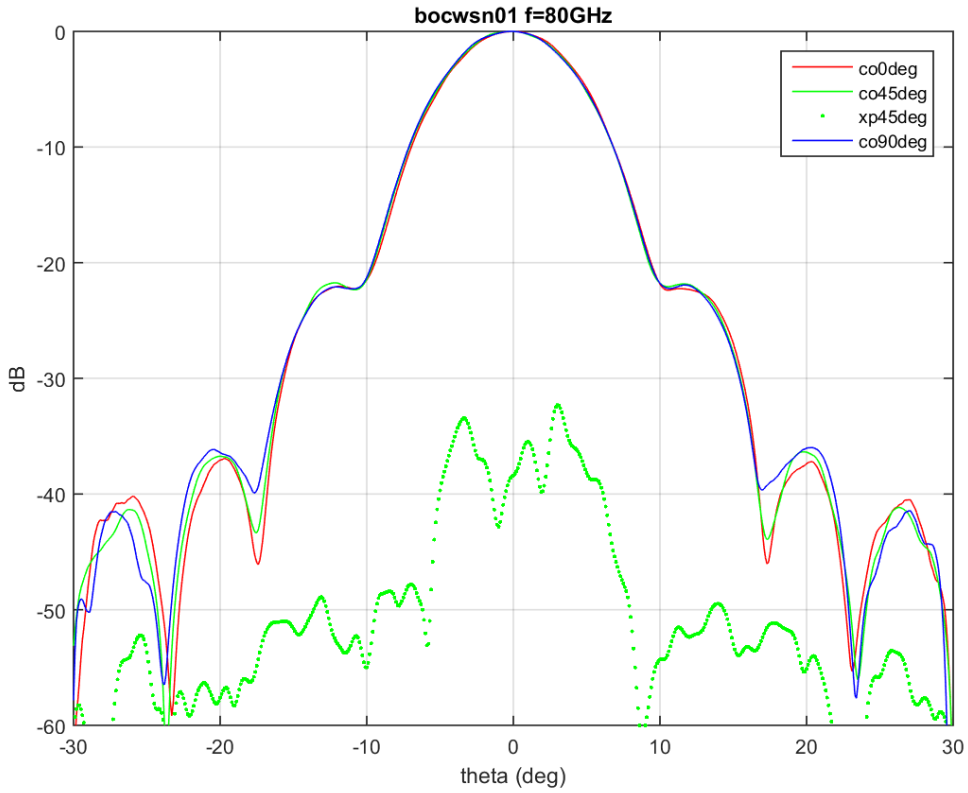
bocwsn01 f=80GHz
co0deg
co45deg
xp45deg
co90deg
dB
theta (deg)
0
-10
-20
-30
-40
-50
-60
-30
-20
-10
0
10
20
30

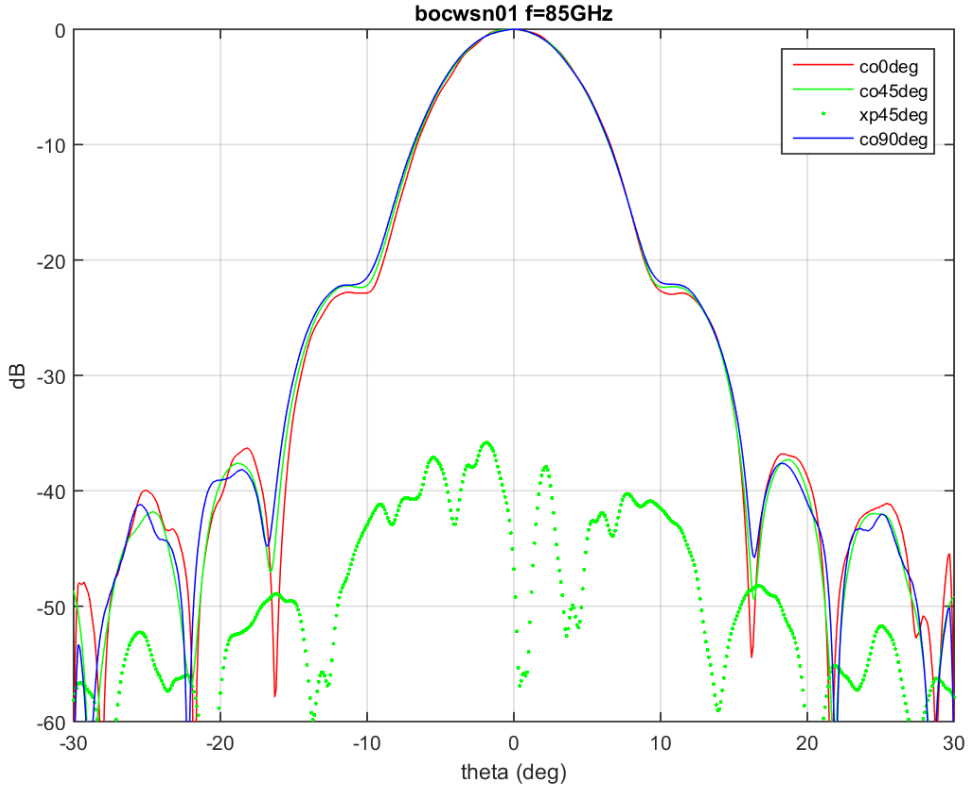
bocwsn01 f=85GHz
co0deg
co45deg
xp45deg
co90deg
dB
theta (deg)
0
-10
-20
-30
-40
-50
-60
-30
-20
-10
0
10
20
30

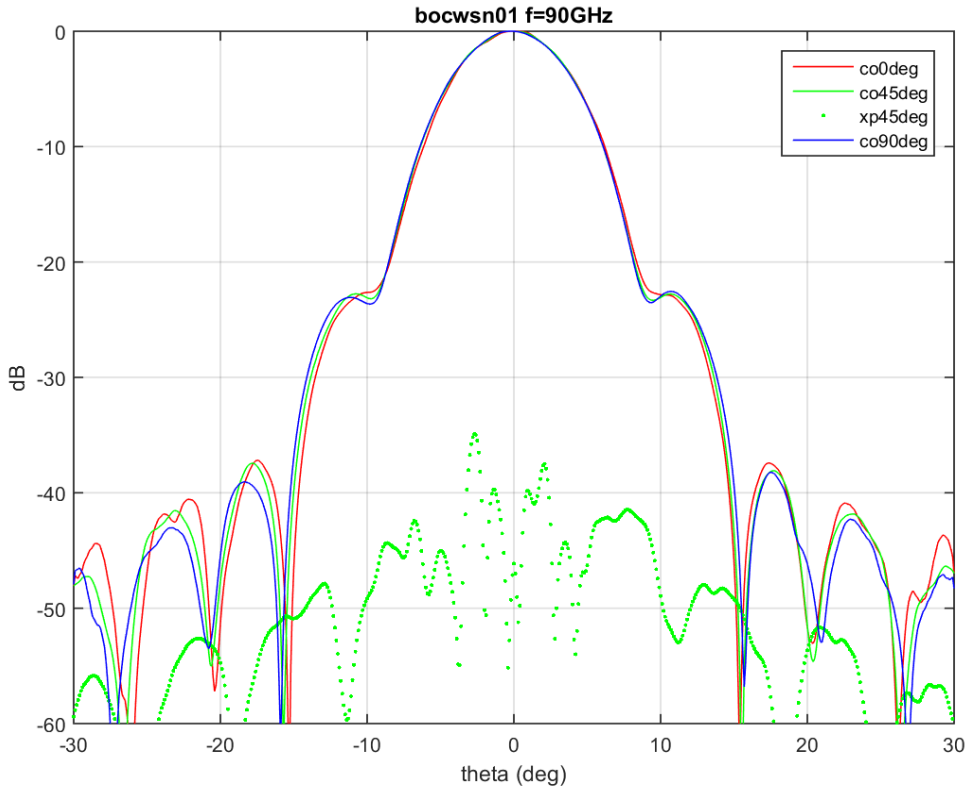
bocwsn01 f=90GHz
co0deg
co45deg
xp45deg
co90deg
dB
theta (deg)
0
-10
-20
-30
-40
-50
-60
-30
-20
-10
0
10
20
30

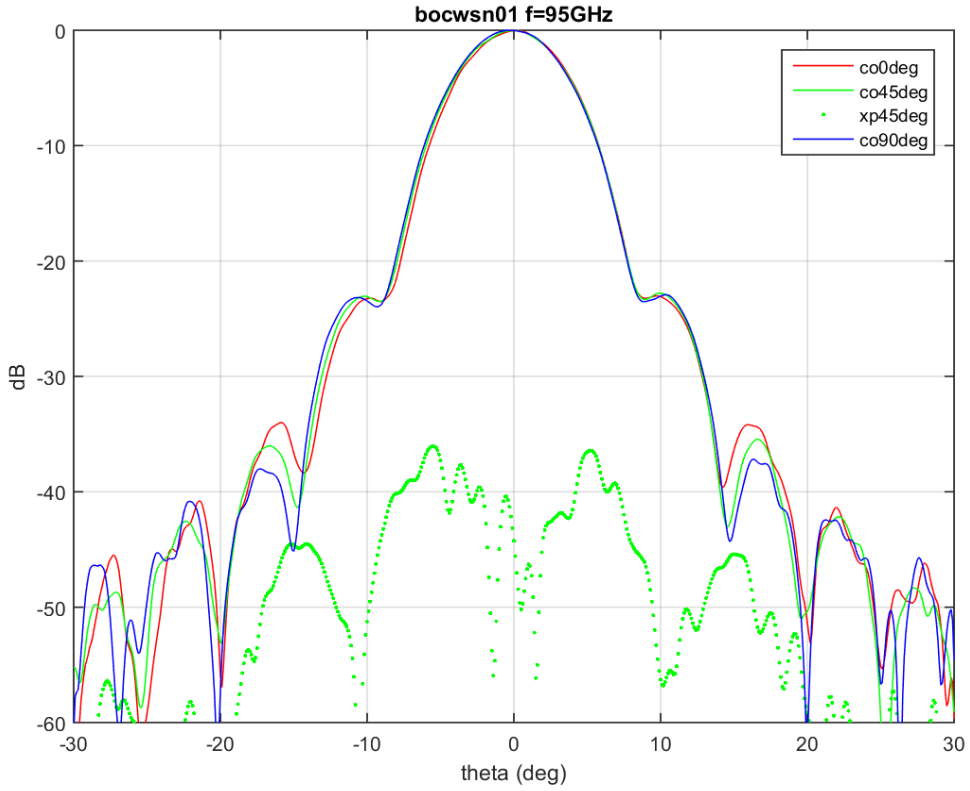
bocwsn01 f=95GHz
co0deg
co45deg
xp45deg
co90deg
dB
theta (deg)
0
-10
-20
-30
-40
-50
-60
-30
-20
-10
0
10
20
30

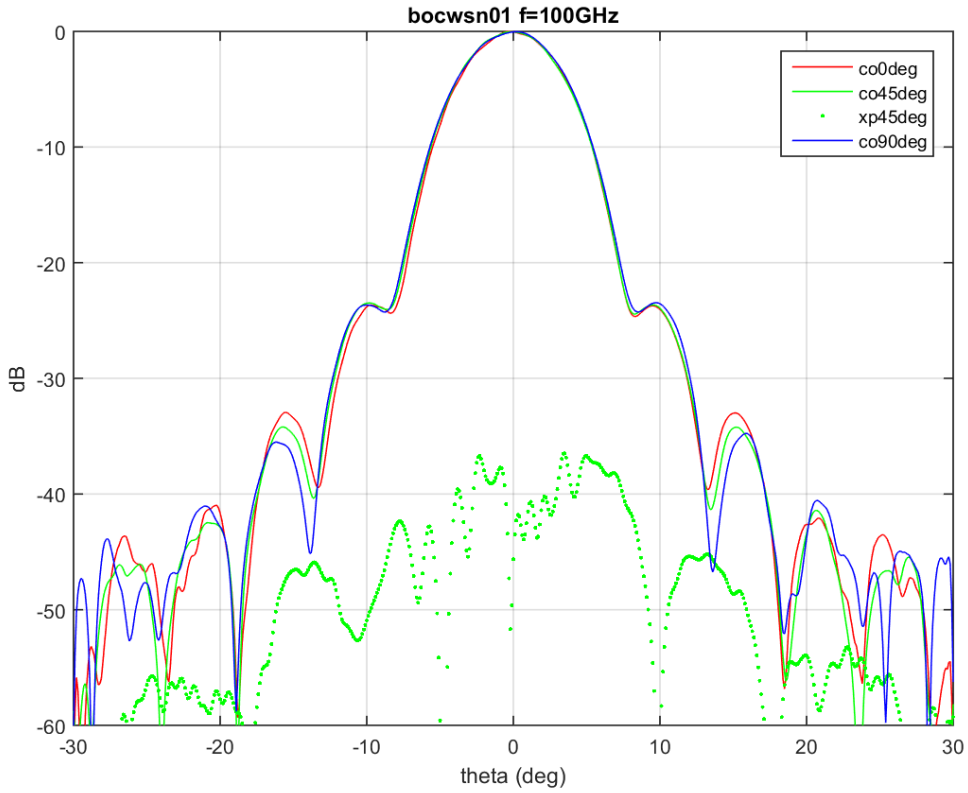
bocwsn01 f=100GHz
co0deg
co45deg
xp45deg
co90deg
dB
theta (deg)
0
-10
-20
-30
-40
-50
-60
-30
-20
-10
0
10
20
30

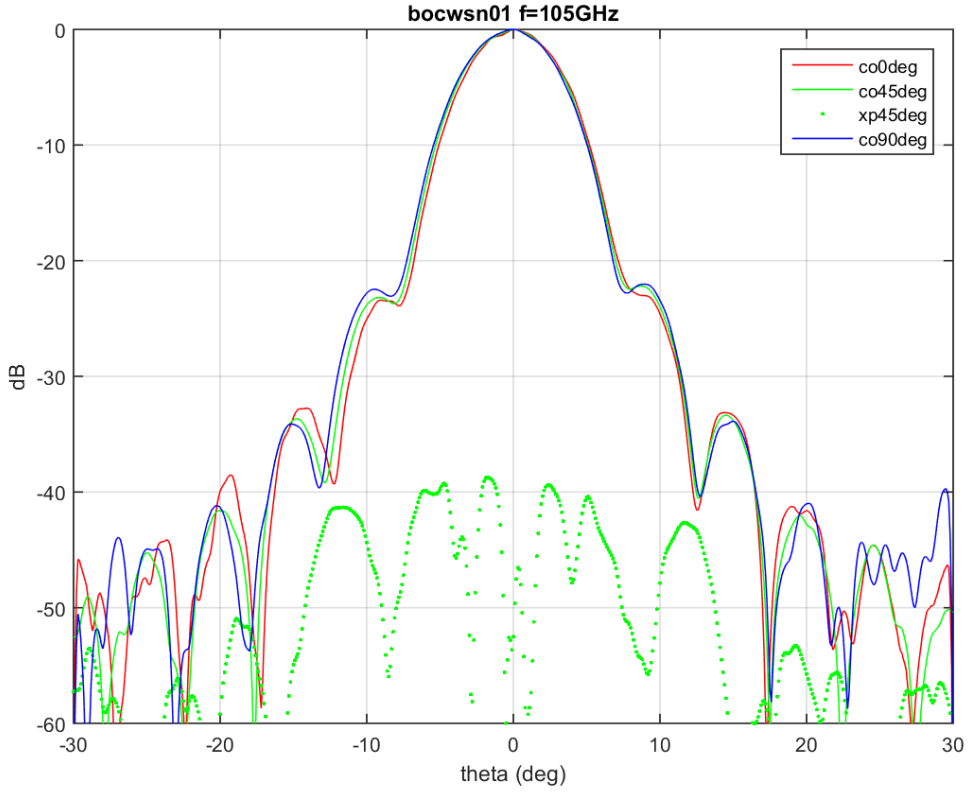
bocwsn01 f=105GHz
co0deg
co45deg
xp45deg
co90deg
dB
theta (deg)
0
-10
-20
-30
-40
-50
-60
-30
-20
-10
0
10
20
30

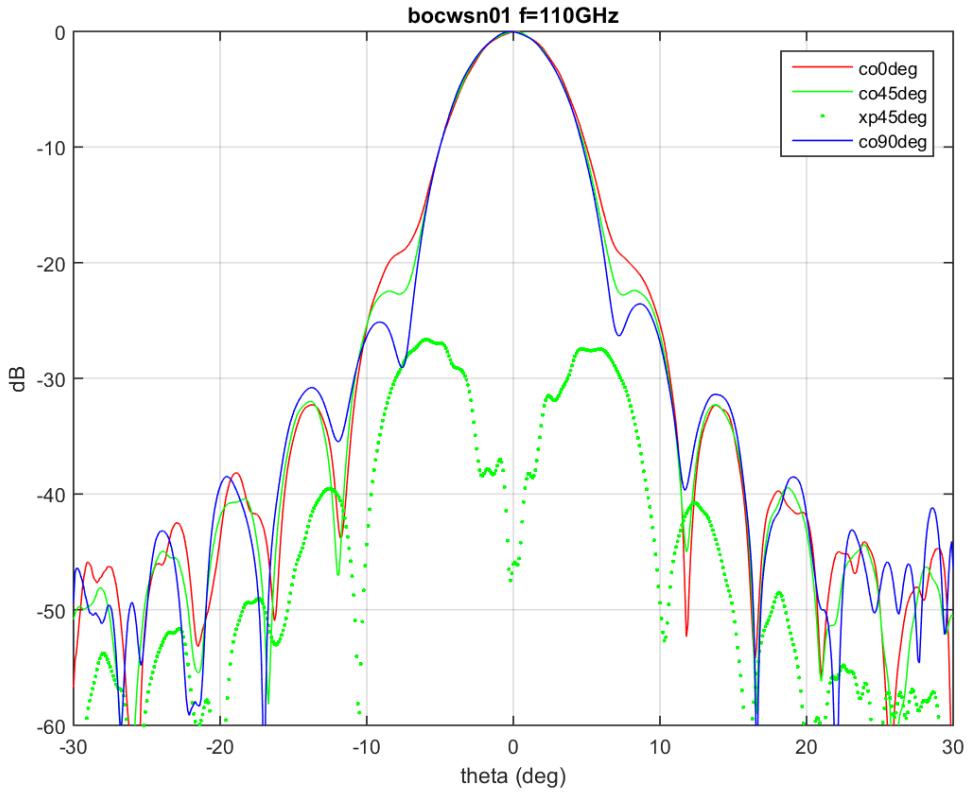
bocwsn01 f=110GHz
co0deg
co45deg
xp45deg
co90deg
dB
theta (deg)
0
-10
-20
-30
-40
-50
-60
-30
-20
-10
0
10
20
30

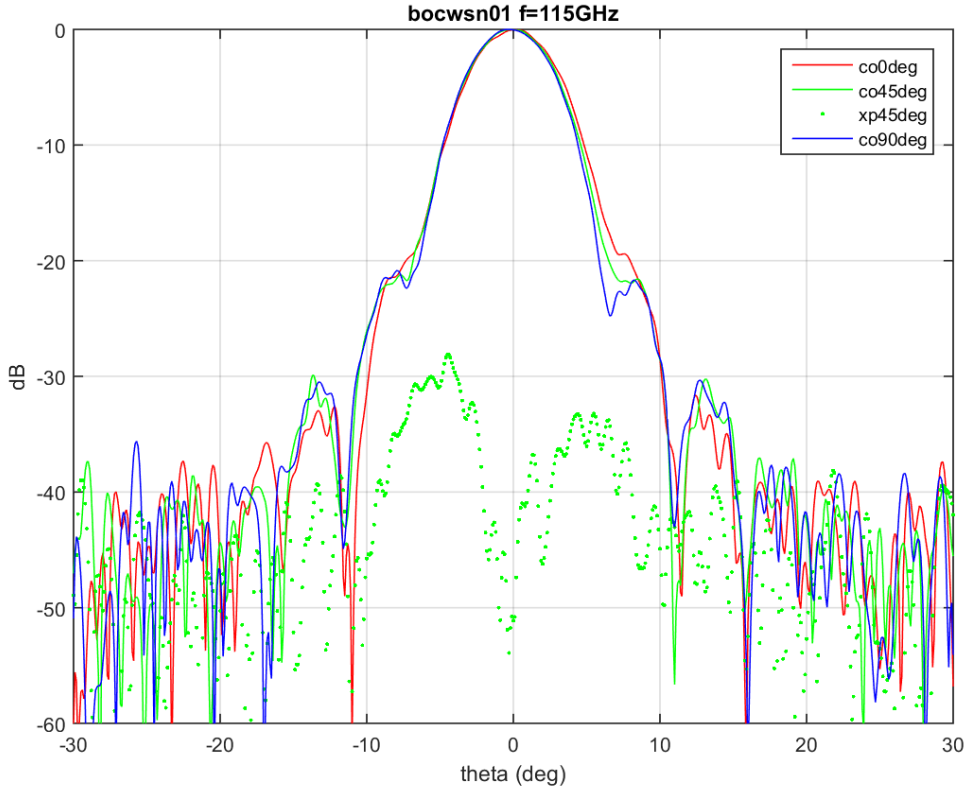
bocwsn01 f=115GHz
co0deg
co45deg
xp45deg
co90deg
dB
theta (deg)
0
-10
-20
-30
-40
-50
-60
-30
-20
-10
0
10
20
30

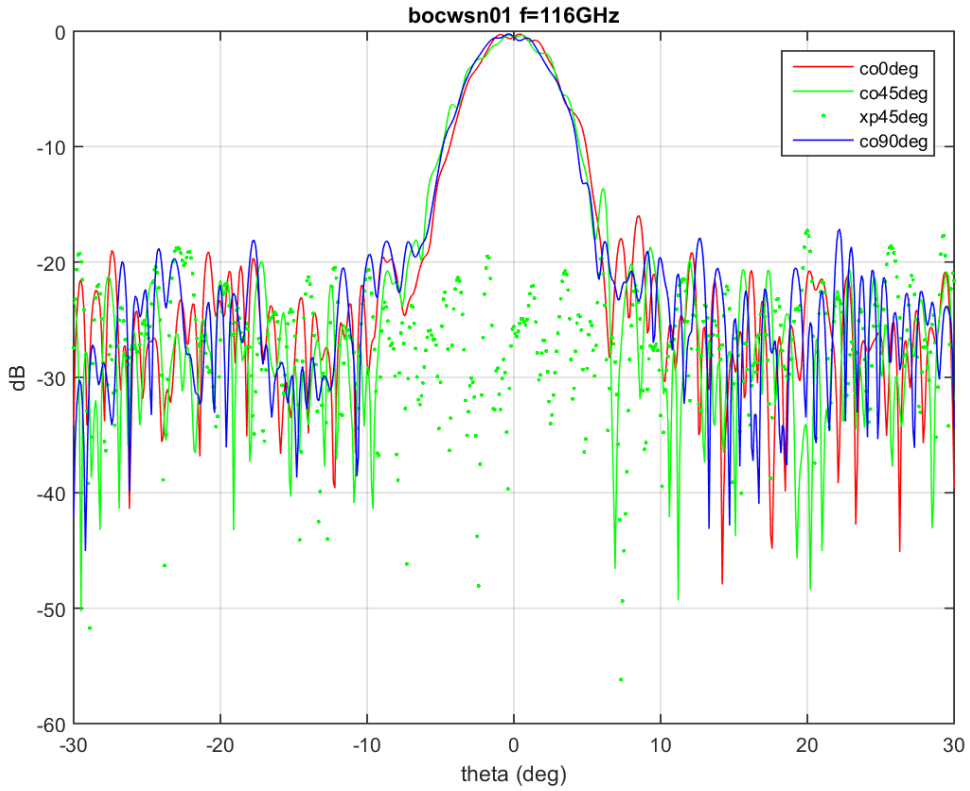
bocwsn01 f=116GHz
co0deg
co45deg
xp45deg
co90deg
dB
theta (deg)
0
-10
-20
-30
-40
-50
-60
-30
-20
-10
0
10
20
30

Appendix F. W-band radiation patterns sn02

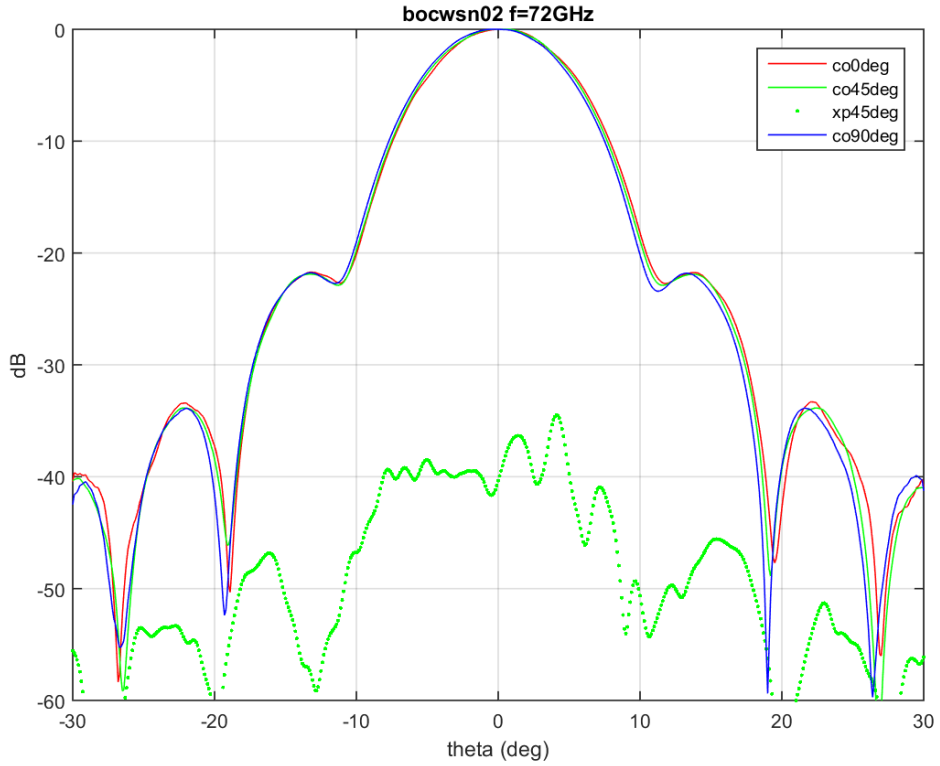

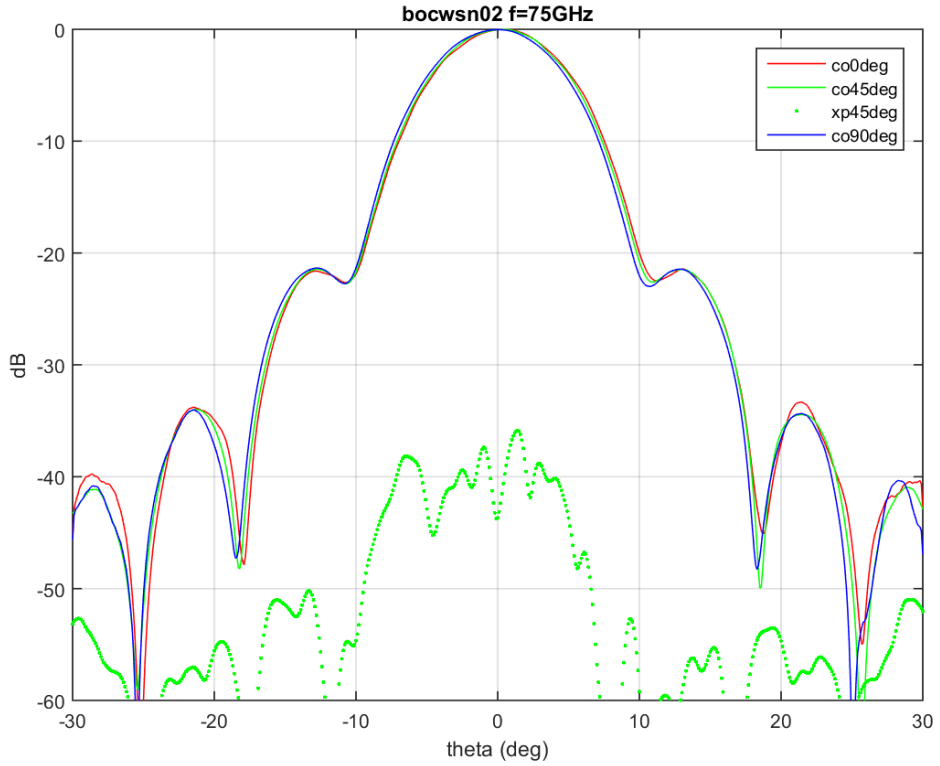

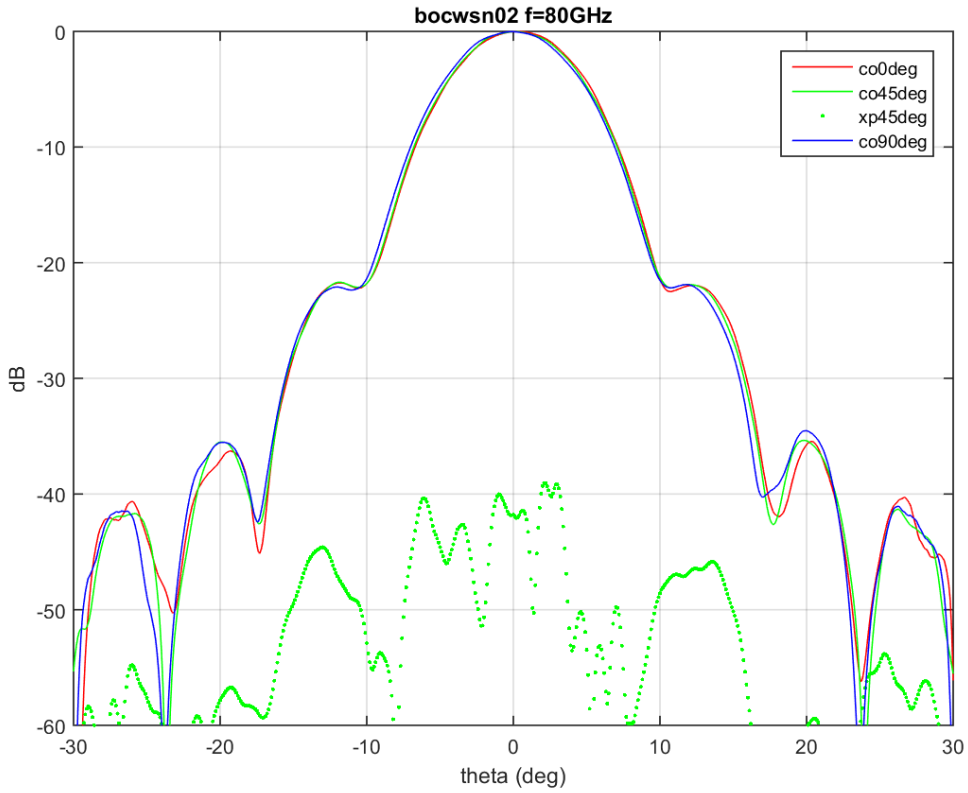
bocwsn02 f=80GHz
co0deg
co45deg
xp45deg
co90deg
dB
theta (deg)
0
-10
-20
-30
-40
-50
-60
-30
-20
-10
0
10
20
30

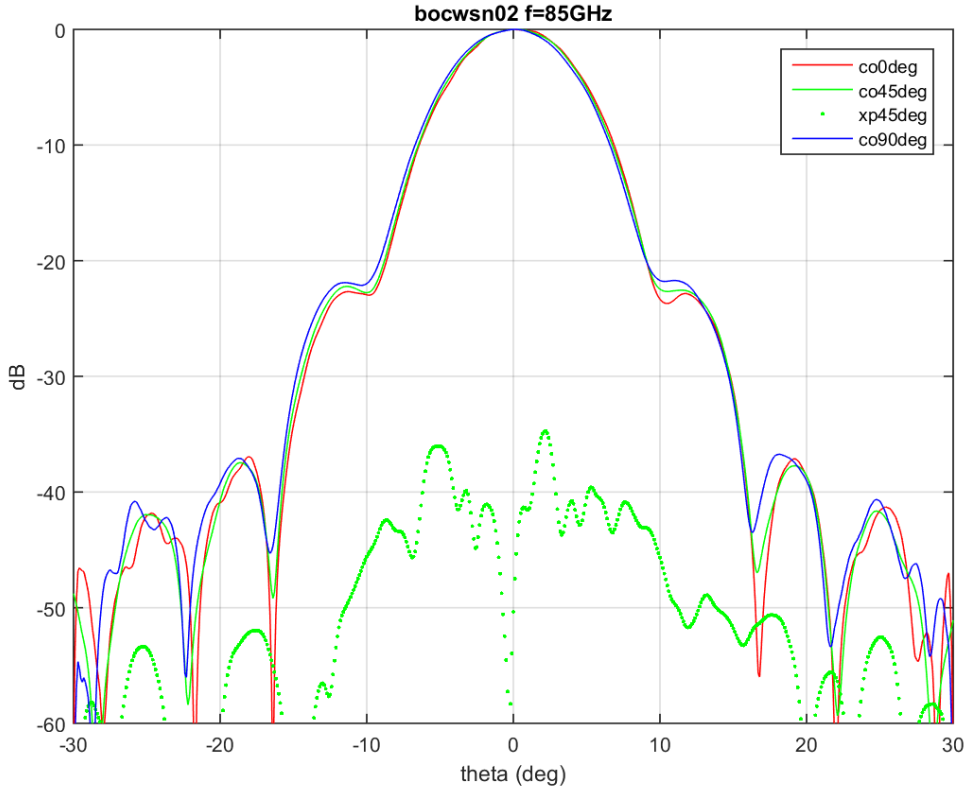
bocwsn02 f=85GHz
co0deg
co45deg
xp45deg
co90deg
dB
theta (deg)
0
-10
-20
-30
-40
-50
-60
-30
-20
-10
0
10
20
30

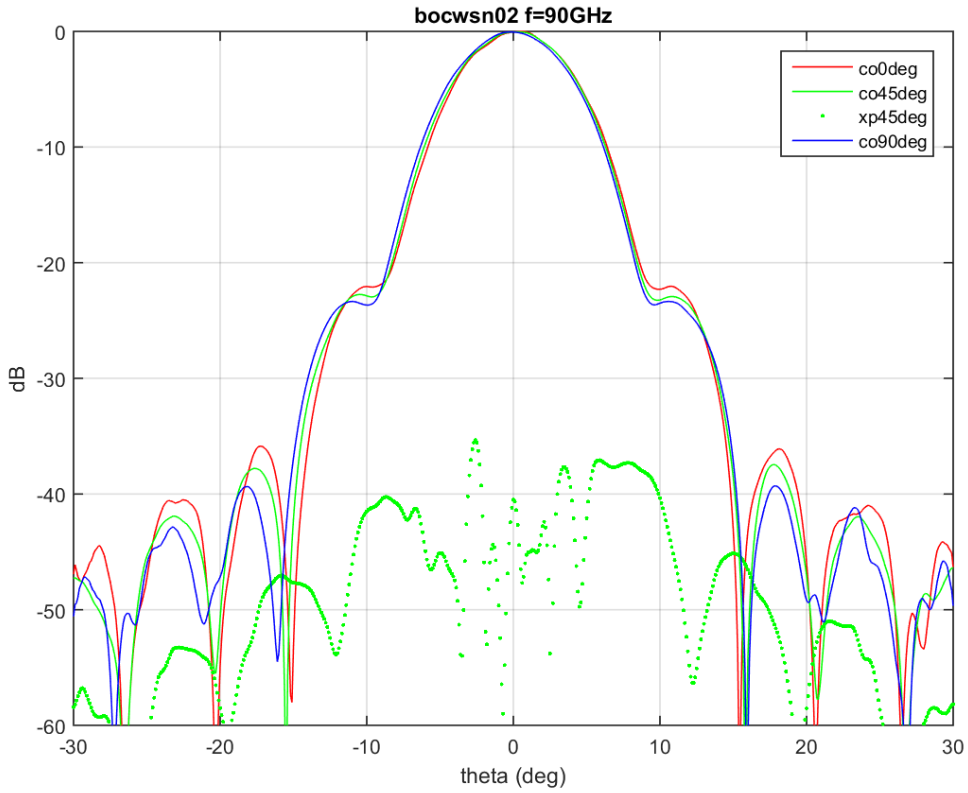
bocwsn02 f=90GHz
co0deg
co45deg
xp45deg
co90deg
dB
theta (deg)
0
-10
-20
-30
-40
-50
-60
-30
-20
-10
0
10
20
30

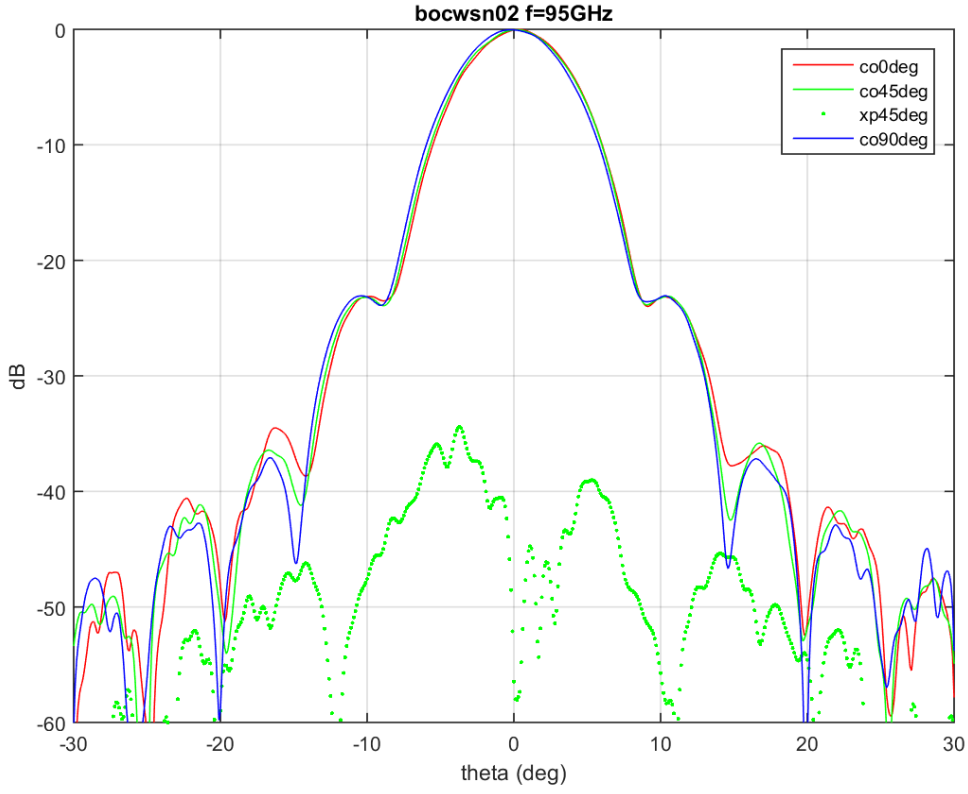
bocwsn02 f=95GHz
co0deg
co45deg
xp45deg
co90deg
dB
theta (deg)
0
-10
-20
-30
-40
-50
-60
-30
-20
-10
0
10
20
30

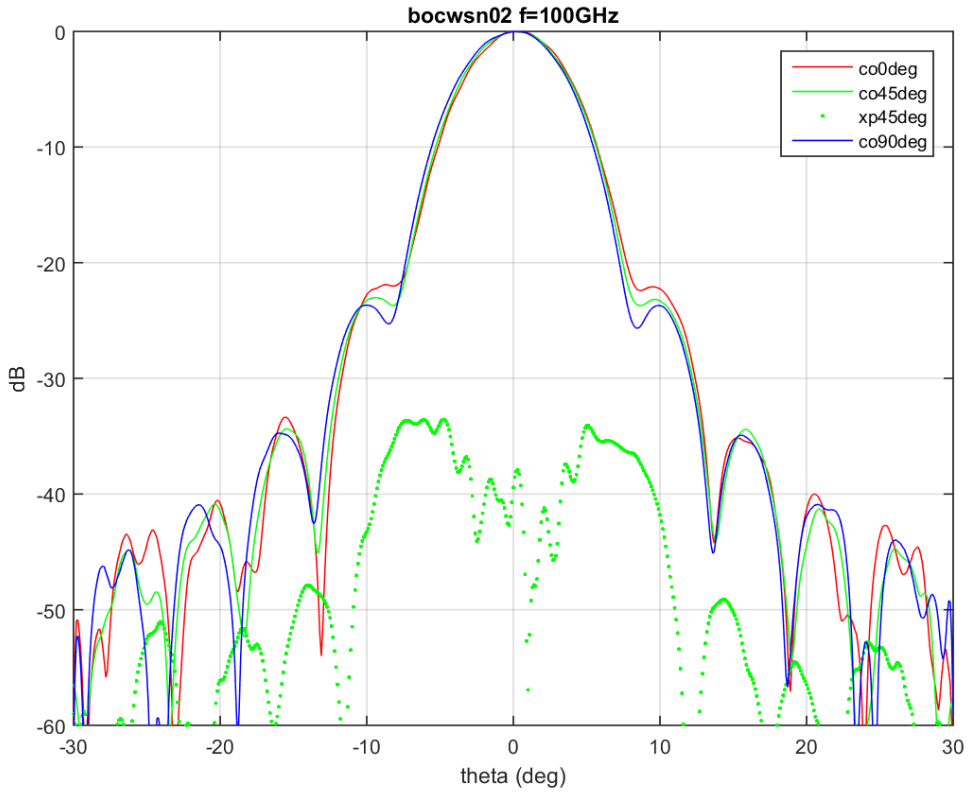
bocwsn02 f=100GHz
co0deg
co45deg
xp45deg
co90deg
dB
theta (deg)
0
-10
-20
-30
-40
-50
-60
-30
-20
-10
0
10
20
30

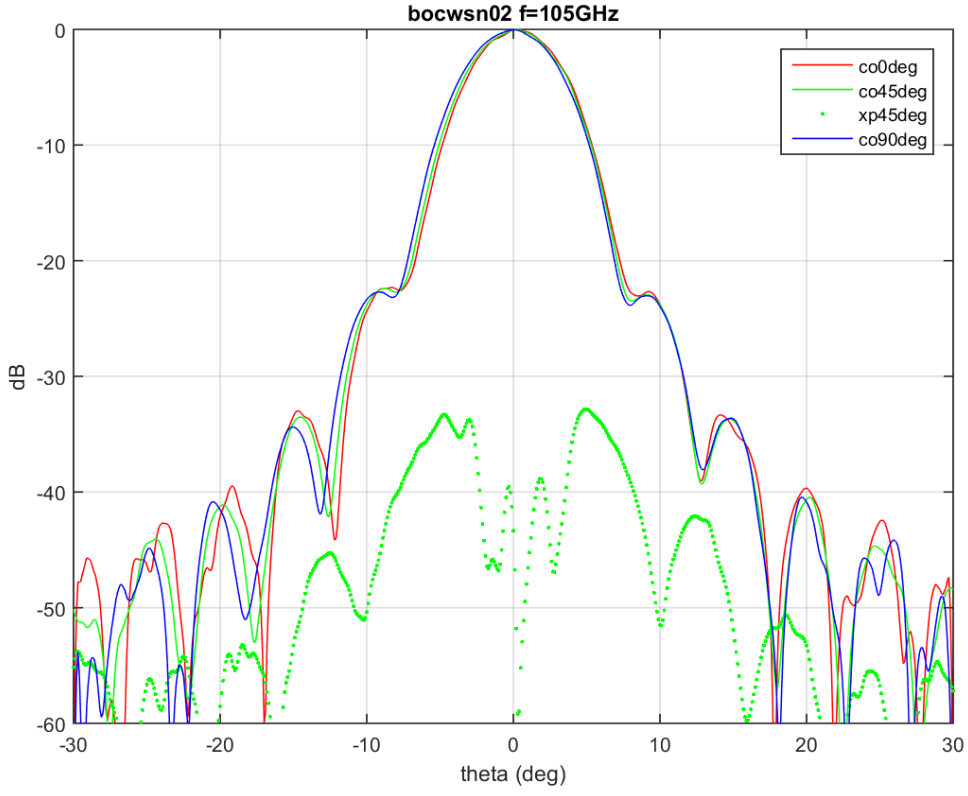
bocwsn02 f=105GHz
co0deg
co45deg
xp45deg
co90deg
dB
theta (deg)
0
-10
-20
-30
-40
-50
-60
-30
-20
-10
0
10
20
30

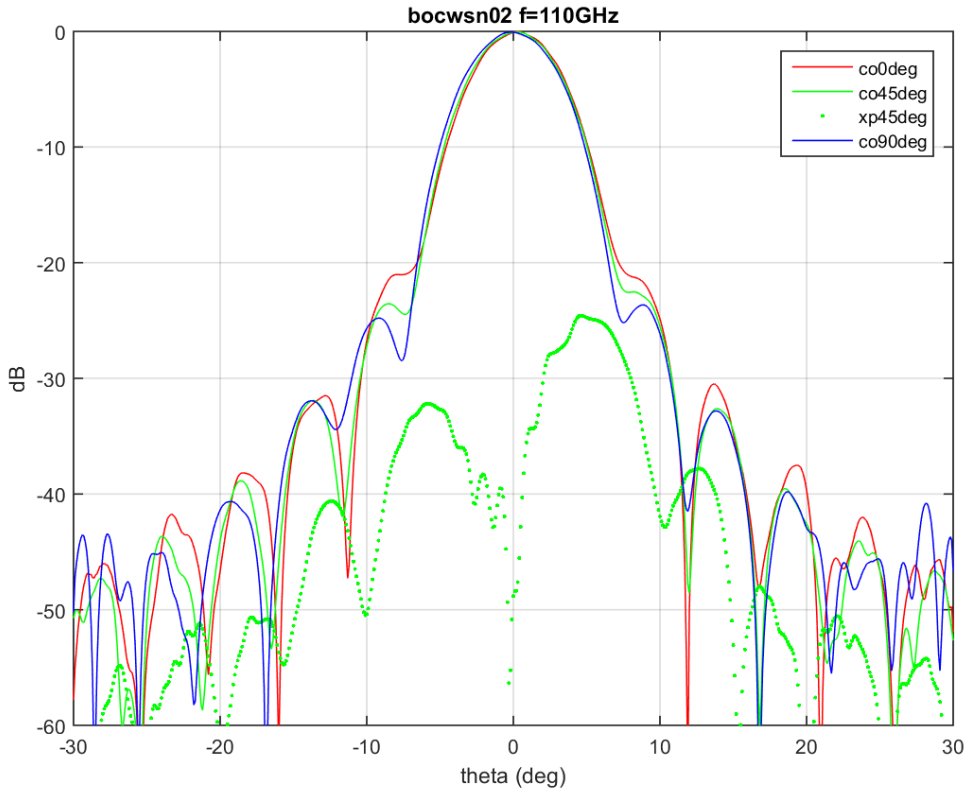
bocwsn02 f=110GHz
co0deg
co45deg
xp45deg
co90deg
dB
theta (deg)
0
-10
-20
-30
-40
-50
-60
-30
-20
-10
0
10
20
30

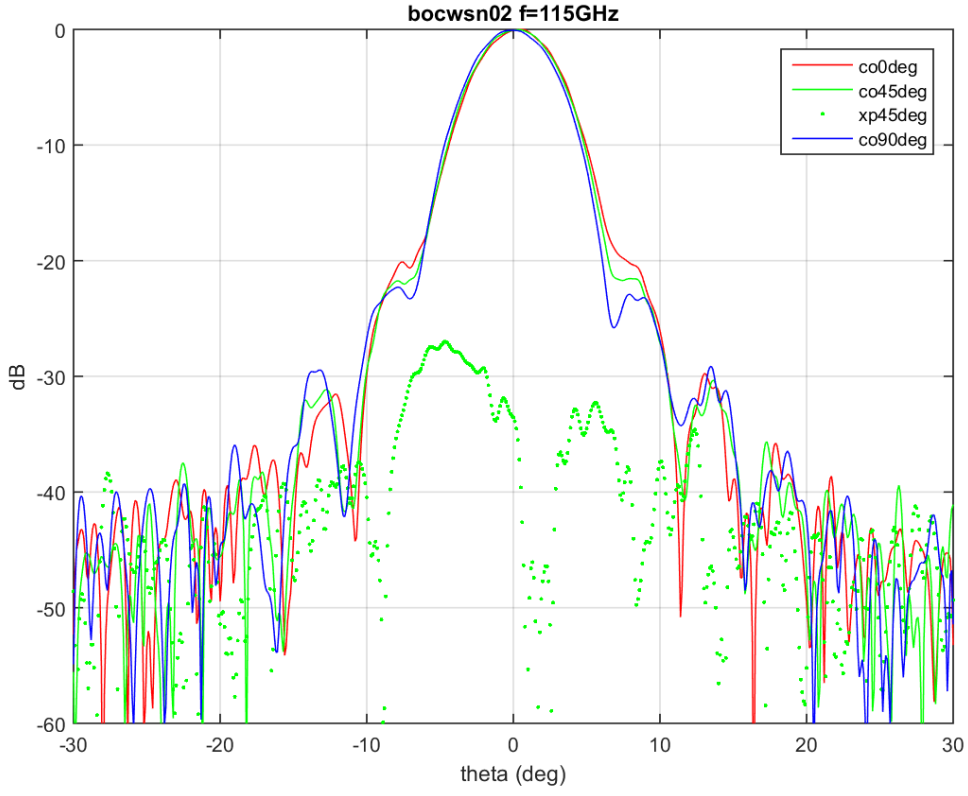
bocwsn02 f=115GHz
co0deg
co45deg
xp45deg
co90deg
dB
theta (deg)
0
-10
-20
-30
-40
-50
-60
-30
-20
-10
0
10
20
30

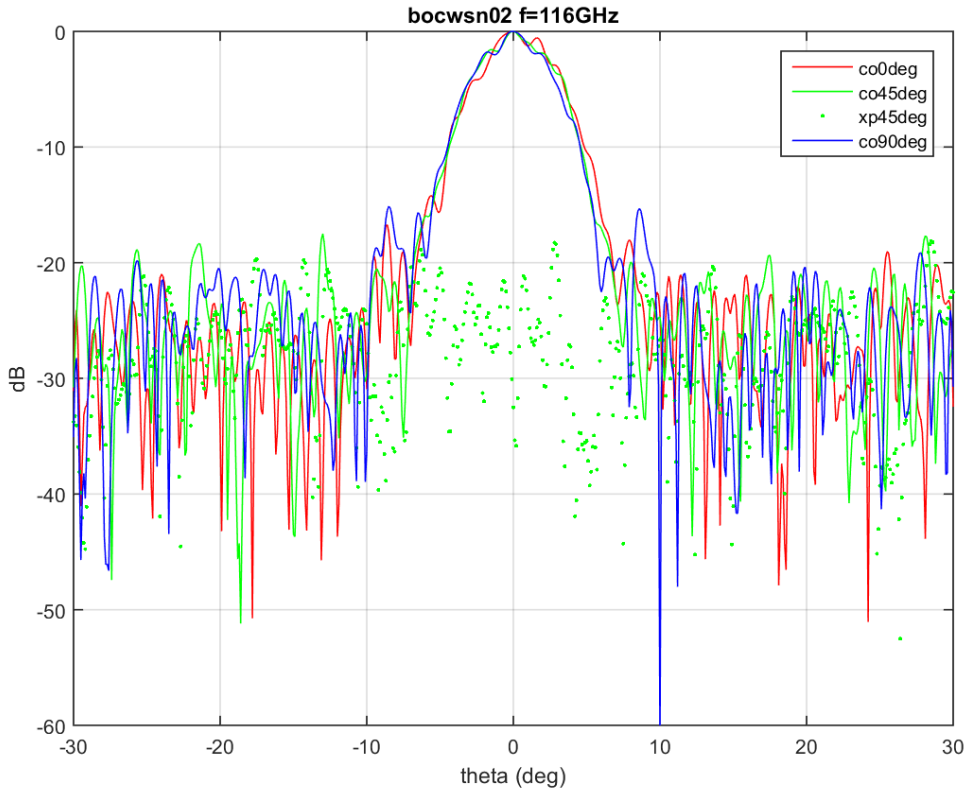
bocwsn02 f=116GHz
co0deg
co45deg
xp45deg
co90deg
dB
theta (deg)
0
-10
-20
-30
-40
-50
-60
-30
-20
-10
0
10
20
30